CHATER IV

RESULTS AND DISCUSSION

In the present study, we studied the molecular mechanism of hydrogen release from the borane amine (BH_3NH_3), alane amine (AlH_3NH_3), borane phosphine (BH_3PH_3) and alane phosphine (AlH_3PH_3) in systems without and with the borane (BH_3), ammonia (NH_3), alane (AlH_3) and phosphine (PH_3).

All energies, rate constant and equilibrium constant presented in this discussion were calculated at the MP2/6-311++G(d,p) level. Due to the calculated results from B3LYP/6-311++G(d,p) corresponds to those from MP2/6-311++G(d,p) level. The calculated results and discussion of each system described below:

4.1 Molecular mechanism of hydrogen release from BH_3NH_3 system

Table 4.1 lists the relative energies, rate constants and thermodynamic properties calculated at the MP2/6-311++G(d,p) and B3LYP/6-311++G(d,p) (in parenthesis) levels of theory for hydrogen release from the BH_3NH_3 without and with the BH_3, NH_3, AlH_3 and PH_3. The reaction pathways for hydrogen release from the BH_3NH_3 system are shown in Figures 4.1-4.5.

4.1.1 Reaction pathway for synthesis of BH_3NH_3 and hydrogen release from BH_3NH_3

The schematic energy profile for hydrogen release from the borane amine without the BH_3, NH_3, AlH_3 and PH_3 is shown in Figure 4.1. The relative energies calculated at the MP2/6-311++G(d,p) and B3LYP/6-311++G(d,p) (in parenthesis) levels of theory for hydrogen release from the BH_3NH_3 are listed in Table 4.1. The reaction pathway for hydrogen release from the BH_3NH_3 is composed of two reaction steps. The first step is the barrierless reaction and the spontaneous and exothermic reaction. The second step is the rate-determining step. The transition state structure, **tsba** for loss of hydrogen from the BH_3NH_3 is similar to that for loss of hydrogen from the C_2H_6 [13]. The shape and geometrical parameter for **tsba** is shown in Figure

A-1(a), one H-atom from BH_3 and other H-atom from NH_3 will eventually form the hydrogen molecule. The H–H distance of 0.99 Å, see Figure A-1(a) is substantially shorter than that of 1.2 Å in the transition state structure of ethane [13]. The energy barrier of **tsba** was calculated to be 36.47 kcal/mol.

We performed a kinetic analysis using the thermodynamic formulation (TST, transition state theory) and included a tunneling correction from the Wigner [19] expression, given by equations (3.43) and (3.44). For hydrogen elimination, the rate constant, k is 2.52×10^{-13} s^{-1}, in gas phase. The reaction is exothermic by 7.92 kcal/mol. In addition, we performed the equilibrium constant using by equation (3.45). The equilibrium constant (K) for hydrogen release from BH_3NH_3 is 1.27×10^{11}.

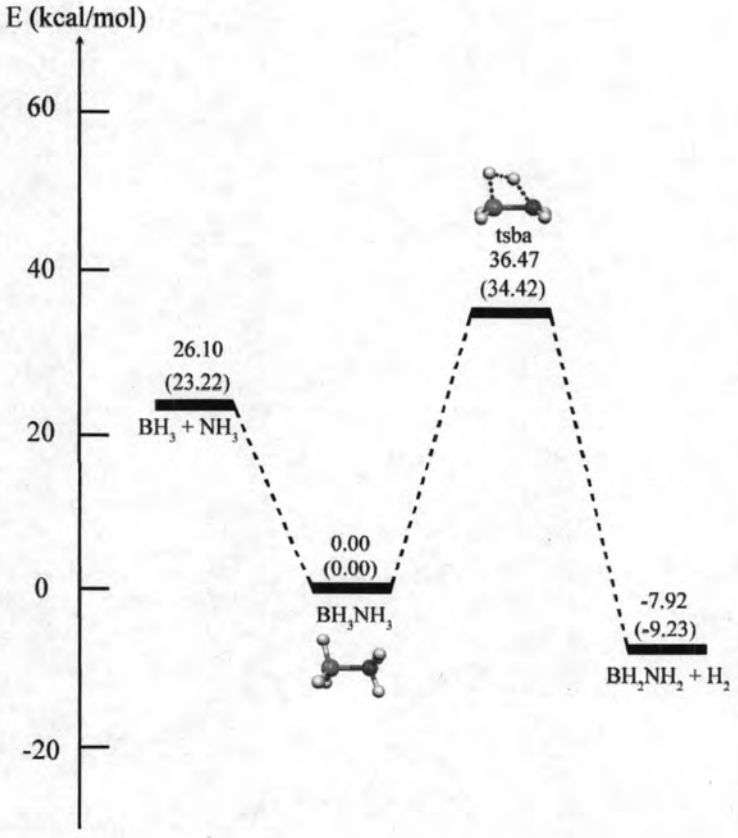

Figure 4.1 Reaction pathway for synthesis of BH_3NH_3 and hydrogen release from BH_3NH_3. Relative energies in kcal/mol computed at the MP2/6-311++G(d,p) and B3LYP/6-311++G(d,p) (in the parenthesis) levels of theory.

Table 4.1 Relative energies, rate constants and thermodynamic properties of hydrogen release from BH_3NH_3 without and with BH_3, NH_3, AlH_3 or PH_3 catalyst, computed at the B3LYP/6-311++G(d,p) (in the parenthesis) and MP2/6-311++G(d,p) levels of theory

Reaction	$\Delta^{\ddagger}E^{a,b}$	$k_{298}{}^{c}$	ΔE^{a}	$\Delta H_{298}{}^{a}$	$\Delta G_{298}{}^{a}$	K_{298}
BH_3NH_3 reactant:						
$BH_3+NH_3 \rightarrow BH_3NH_3$	-	-	-26.10	-27.92	-17.84	1.19×10^{13}
	-	-	(-23.22)	(-25.03)	(-14.98)	(9.51×10^{10})
$BH_3NH_3 \rightarrow$ **tsba** $\rightarrow BH_2NH_2+H_2$	36.47	2.52×10^{-13}	-7.92	-6.15	-15.15	1.27×10^{11}
	(34.42)	(7.46×10^{-12})	(-9.23)	(-7.52)	(-16.42)	(1.08×10^{12})
BH_3NH_3 and BH_3 reactants:						
$BH_3NH_3+BH_3 \rightarrow BH_3NH_3\cdots BH_3$	-	-	-16.18	-17.35	-8.05	7.98×10^{5}
	-	-	(-13.97)	(-14.97)	(-6.17)	(3.35×10^{4})
$BH_3NH_3\cdots BH_3 \rightarrow$ **tsba-BN** $\rightarrow BH_2NH_2+H_2+BH_3$	23.62	2.37×10^{-5}	-7.92	11.20	-7.10	1.60×10^{5}
	(20.84)	(1.95×10^{-3})	(-9.23)	(7.45)	(-10.24)	(3.22×10^{7})
$BH_3NH_3\cdots BH_3 \rightarrow$ **tsba-BH_3** $\rightarrow NH_2BH_2BH_3$(ring)$+H_2$	45.36	2.25×10^{-20}	-36.75	-19.64	-26.01	1.18×10^{19}
	(45.10)	(8.11×10^{-21})	(-31.87)	(-17.13)	(-23.43)	(1.50×10^{17})
$BH_3NH_3\cdots BH_3 \rightarrow$ **tsba-BB** $\rightarrow BH_2NH_2+H_2+BH_3$	65.18	3.36×10^{-35}	-7.92	11.20	-7.10	1.60×10^{5}
	(58.21)	(2.55×10^{-30})	(-9.23)	(7.45)	(-10.24)	(3.22×10^{7})
BH_3NH_3 and NH_3 reactants:						
$BH_3NH_3+NH_3 \rightarrow BH_3NH_3\cdots NH_3$	-	-	-8.48	-8.82	-1.75	1.93×10^{1}
	-	-	(-7.26)	(-7.58)	(-0.51)	(2.38)
$BH_3NH_3\cdots NH_3 \rightarrow$ **tsba-NN** $\rightarrow BH_2NH_2+H_2+NH_3$	106.50	5.34×10^{-67}	-7.92	2.67	-13.40	6.61×10^{9}
	(99.45)	(1.66×10^{-61})	(-9.23)	(0.06)	(-15.90)	(4.54×10^{11})
$BH_3NH_3\cdots NH_3 \rightarrow$ **tsba-NH_3** $\rightarrow BH_2NH_2+H_2+NH_3$	40.74	1.53×10^{-16}	-7.92	2.67	-13.40	6.61×10^{9}
	(38.43)	(7.75×10^{-15})	(-9.23)	(0.06)	(-15.90)	(4.54×10^{11})
$BH_3NH_3\cdots NH_3 \rightarrow$ **tsba-NB** $\rightarrow BH_2NH_2+H_2+NH_3$	30.30	1.81×10^{-11}	-7.92	2.67	-13.40	6.61×10^{9}
	(29.01)	(4.05×10^{-10})	(-9.23)	(0.06)	(-15.90)	(4.54×10^{11})
BH_3NH_3 and AlH_3 reactants:						
$BH_3NH_3+AlH_3 \rightarrow BH_3NH_3\cdots AlH_3$	-	-	-16.36	-17.26	-8.03	7.65×10^{5}
	-	-	(-14.30)	(-15.14)	(-6.06)	(2.79×10^{4})
$BH_3NH_3\cdots AlH_3 \rightarrow$ **tsba-AlN** $\rightarrow NH_2BH_2AlH_3$(ring)$+H_2$	18.51	1.30×10^{-1}	-36.67	-19.10	-26.28	1.85×10^{19}
	(17.38)	(9.27×10^{-1})	(-31.56)	(-16.10)	(-23.14)	(9.17×10^{16})
$BH_3NH_3\cdots AlH_3 \rightarrow$ **tsba-AlH_3** $\rightarrow NH_2BH_2AlH_3$(ring)$+H_2$	42.78	6.66×10^{-19}	-36.67	-19.10	-26.28	1.85×10^{19}
	(42.25)	(2.50×10^{-18})	(-31.56)	(-16.10)	(-23.14)	(9.17×10^{16})
$BH_3NH_3\cdots AlH_3 \rightarrow$ **tsba-AlB** $\rightarrow BH_2NH_2+H_2+AlH_3$	61.49	2.00×10^{-32}	-7.92	11.11	-7.12	1.67×10^{5}
	(54.89)	(1.28×10^{-27})	(-9.23)	(7.62)	(-10.35)	(3.87×10^{7})
BH_3NH_3 and PH_3 reactants:						
$BH_3NH_3+PH_3 \rightarrow BH_3NH_3\cdots PH_3$	-	-	-38.30	-38.12	-32.26	4.47×10^{23}
	-	-	(-35.10)	(-35.29)	(-28.90)	(1.53×10^{21})
$BH_3NH_3\cdots PH_3 \rightarrow$ **tsba-PN** $\rightarrow BH_2NH_2+H_2+PH_3$	61.00	3.37×10^{-34}	-7.92	31.97	17.11	2.85×10^{-13}
	(55.12)	(1.03×10^{-29})	(-9.23)	(27.76)	(12.48)	(7.06×10^{-10})
$BH_3NH_3\cdots PH_3 \rightarrow$ **tsba-PH_3** $\rightarrow BH_2NH_2+H_2+PH_3$	38.25	1.36×10^{-14}	-7.92	31.97	17.11	2.85×10^{-13}
	(35.87)	(5.23×10^{-12})	(-9.23)	(27.76)	(12.48)	(7.06×10^{-10})
$BH_3NH_3\cdots PH_3 \rightarrow$ **tsba-PB** $\rightarrow BH_2NH_2+H_2+PH_3$	45.83	2.07×10^{-22}	-7.92	31.97	17.11	2.85×10^{-13}
	(47.83)	(1.64×10^{-24})	(-9.23)	(27.76)	(12.48)	(7.06×10^{-10})

[a] In kcal/mol.
[b] Activation energy.
[c] In s^{-1}

4.1.2 Reaction pathway for hydrogen release from BH_3NH_3 in the presence of BH_3

The potential energy profile for hydrogen release from the BH_3NH_3 in the presence of BH_3, computed at the MP2/6-311++G(d,p) and B3LYP/6-311++G(d,p) (in parenthesis) are shown in Figure 4.2. The relative energies, rate constants and thermodynamic properties of hydrogen release system of BH_3NH_3 in the presence of BH_3 are listed in Table 4.1. Figure 4.2 shows that the first step is the complexation of BH_3NH_3 and BH_3 resulting the **ba-com-BH_3**, this step is the barrierless and its reaction is the spontaneous and exothermic process. The second step is composed of three reaction pathways via the transition-state structures **tsba_BN**, **tsba_BH_3** and **tsba_BB** as shown in Figure A-2. The activation energies of three pathways in the second step via **tsba_BN**, **tsba_BH_3** and **tsba_BB** are 23.62, 45.36 and 65.18 kcal/mol, respectively. The most favorable pathway is therefore the pathway via the transition-state structure, **tsba_BN**. The hydrogen release process of the second most favorable pathway via the transition state of **tsba_BH_3** seems to be similar to its corresponding process in system without of any catalyst. This pathway results the three-membered ring, **ba-ring-BH_3** which the BH_3 is never released from its complex-state. Therefore, the BH_3 does not behave as the catalyst.

In the transition-state structure, **tsba_BB** and **tsba_BN**, the reaction pathways via either **tsba_BB** or **tsba_BN** result the same products as BH_2NH_2, H_2 and BH_3. This result is in the agreement with a previous theoretical study [13]. The activation energy of the most favorable path, via the **tsba_BN** is lower than its corresponding hydrogen release compound in system without BH_3 by 12.85 kcal/mol.

The tunneling factor (κ) of the most favorable path based on the Wigner expression, calculated imaginary frequency for **tsba_BN**, $v_i = 810i$ cm^{-1} at the MP2/6-311++G(d,p) level is $\kappa = 1.64$ as listed in Table B-1. Moreover, we can apply the TST theory to predict the rate constant for hydrogen release of **ba-com-BH_3**, via **tsba_BN**. By use of the equations (3.43) and (3.44), the TST rate constant of $k = 2.37\times10^{-5}$ s^{-1} is obtained. The tunneling factors and reaction constants of all hydrogen release compound systems are shown in Tables B-1 and 4.1, respectively. The equilibrium constant (K) calculated from equation (3.45) of the reaction via **tsba-BH_3** is 1.27×10^{11}. It was found that the product **ba-ring-BH_3** is the most favorable product because its structure is more stable than the product BH_2NH_2.

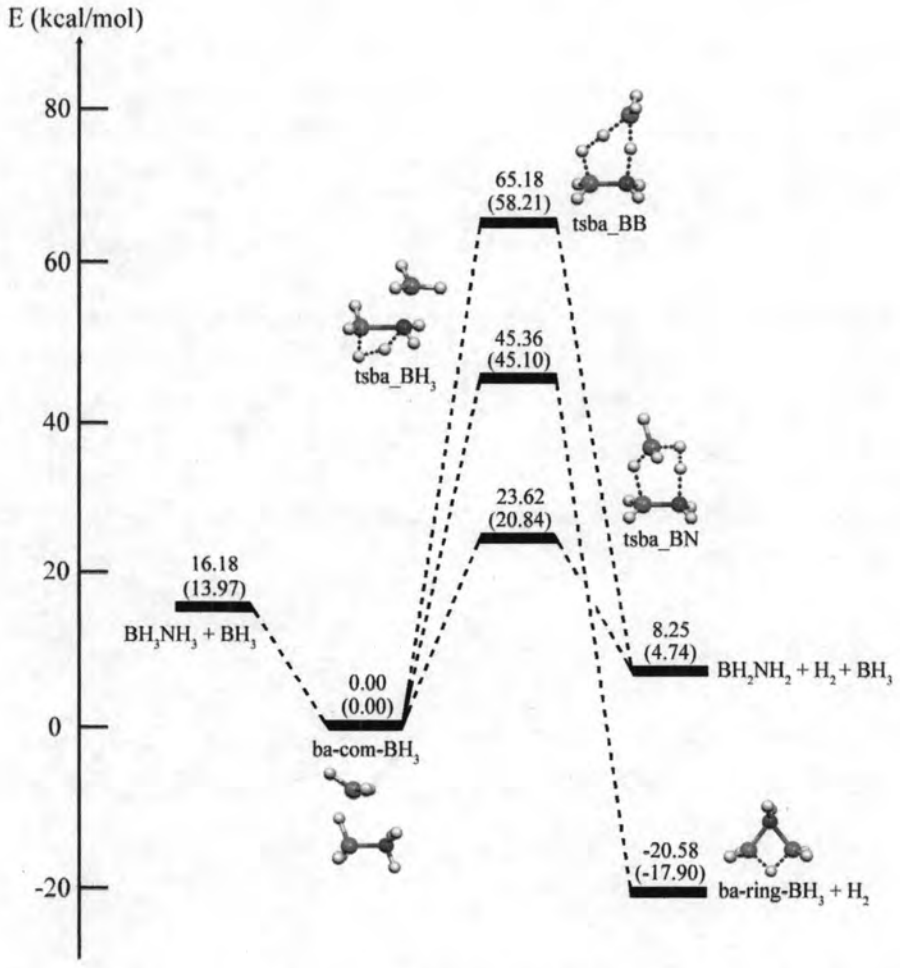

Figure 4.2 Reaction pathways for hydrogen release from BH_3NH_3 in the presence of BH_3. Relative energies in kcal/mol computed at the MP2/6-311++G(d,p) and B3LYP/6-311++G(d,p) (in the parenthesis) levels of theory.

4.1.3 Reaction pathway for hydrogen release from BH_3NH_3 in the presence of NH_3

The reaction pathways for hydrogen release from the BH_3NH_3 with NH_3 are given in Figure 4.3. Table 4.1 lists the relative energies, rate constants and thermodynamic properties of hydrogen release from the BH_3NH_3 in the presence of NH_3. The process of hydrogen release from the BH_3NH_3 with NH_3 is similar to the hydrogen release from the BH_3NH_3 with BH_3 discussed. The first step is the complexation between BH_3NH_3 and NH_3 resulting the **ba-com-NH_3**. The complexation energy of **ba-com-NH_3** is -8.48 kcal/mol. The second step, the transition-state structures have been located via **tsba_NN**, **tsba_NH_3** and **tsba_NB** as shown in Figure A-3. The transition-state structure, **tsba_NH_3** corresponds to the

transition-state structure, **tsba_BH_3** described above, the energy barrier based on the transition-state structure, **tsba_NH_3** of 40.74 kcal/mol is found. The transition-state structures, **tsba_NB** and **tsba_NN** correspond to the processes in which **tsba_BB** and **tsba_BN**, respectively. Relative to the separated reactants, the energy of **tsba_NB** and **tsba_NN** are calculated to be 21.82 kcal/mol and 97.02 kcal/mol, respectively. Thus, the structure of **tsba_NB**, is more stable than of **tsba_NN.** The energy barrier of the transition-state structure, **tsba_NB** represents a reduction of 6.17 kcal/mol with respect to the energy barrier of 36.47 kcal/mol in the monomer via **tsba**, see Figure A-1(a). Three pathways result the same fragmented products as BH_2NH_2, H_2 and NH_3, the energy of reaction was calculated to be -7.92 kcal/mol below the reactants. All reaction energies via **tsba_NN**, **tsba_NH_3** and **tsba_NB** are negative that indicate over all reaction become exothermic processes.

The rate constants of the catalytic processes can be evaluated by equations (3.43) and (3.44). The rate constants via **tsba_NB** and **tsba_NN** are $k = 1.81\times10^{-11}$ s^{-1} and $k = 5.34\times10^{-67}$ s^{-1}, respectively. These values show that the transfer of two H-atoms from the BH_3NH_3 should be significantly faster in **tsba_NB** than in **tsba_NN**. In addition, the tunneling factors (κ) and reaction constants of all hydrogen release compound systems are listed in Tables B-1 and 4.1, respectively.

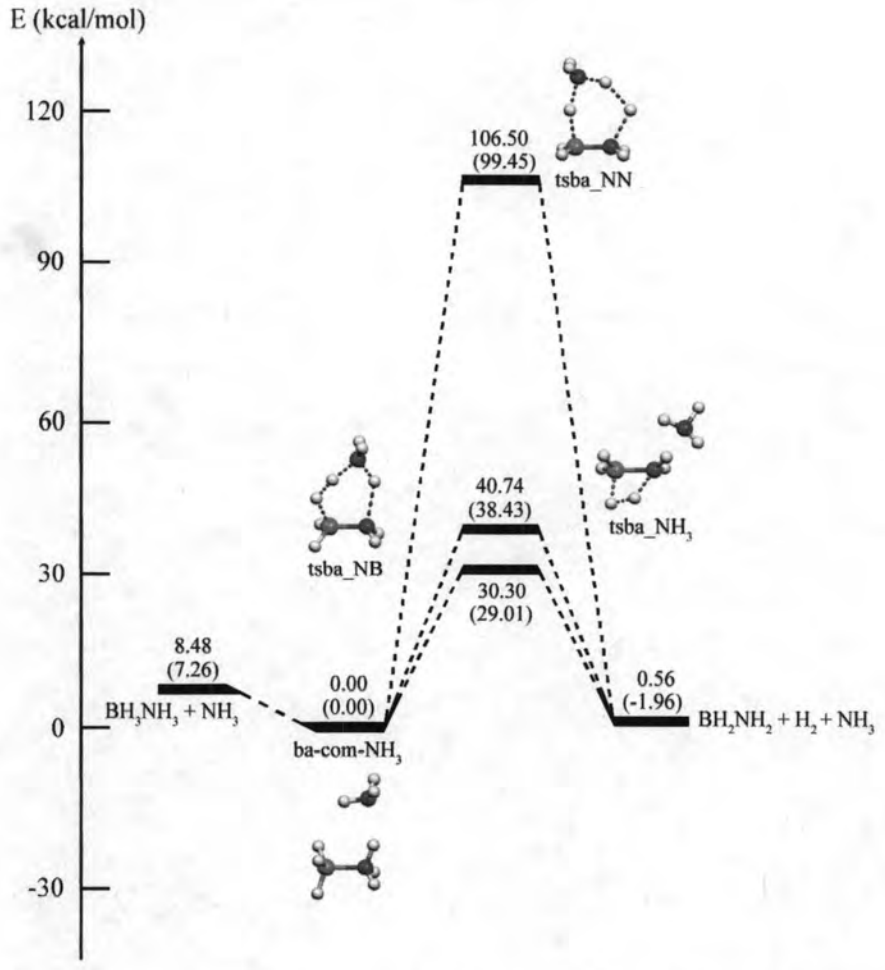

Figure 4.3 Reaction pathways for hydrogen release from BH_3NH_3 in the presence of NH_3. Relative energies in kcal/mol computed at the MP2/6-311++G(d,p) and B3LYP/6-311++G(d,p) (in the parenthesis) levels of theory.

4.1.4 Reaction pathway for hydrogen release from BH_3NH_3 in the presence of AlH_3

We have studied whether an alane molecule could participate as a catalyst. For the BH_3NH_3 + AlH_3 reaction, we located three different transition-state structures, bond length are displayed in Figure A-4. The corresponding energy profile is illustrated in Figure 4.4. The shape and characteristics of the transition-state structures involving AlH_3 are similar in many respects to those involving BH_3 and NH_3 discussed above. The relative energies, rate constants and thermodynamic properties of hydrogen release from the BH_3NH_3 in the presence of AlH_3 computed at the MP2/6-311++G(d,p) and B3LYP/6-311++G(d,p) (in parenthesis) are listed in Table 4.1. The reaction pathways for this system are composed of two reaction steps such as

the hydrogen release from the BH_3NH_3 with BH_3 and NH_3. The first step, BH_3NH_3 + AlH_3 leads to the complex, **ba-com-AlH_3**. The energy of **ba-com-AlH_3** is calculated to be 16.36 kcal/mol. The second step, three transition-state structures for hydrogen release have been found, via **tsba_AlN**, **tsba_AlH_3** and **tsba_AlB** (Figure A-4). In the transition-state structure, **tsba_AlB**, the process via **tsba_AlB** proceeds with high energy because both H-atoms are negatively charged, the repulsion results in a substantial energy barrier of 61.49 kcal/mol. This pathway results the fragmented products, the BH_2NH_2, H_2 and AlH_3. For the transition-state structure, **tsba_AlH_3**, the activation energy is 42.78 kcal/mol. The three-membered ring with Al–H–B bridge is found to be the most stable product, and with the product H_2, this energy reaction is 36.66 kcal/mol below the reactants. The most favorable pathway is therefore the pathway via **tsba_AlN**. The H–H distance of 0.82 Å, see Figure A-4(a) shows that the departing H_2 is formed at the transition state. The energy barrier via **tsba_AlN** is 18.51 kcal/mol. The same separated products as that described above have been generated.

Table 4.1 lists the calculated rate constants, including tunneling correction, using TST for each process in this system from equations (3.43) and (3.44). Table B-1 shows the tunneling factors (κ) for all reaction of hydrogen release from the BH_3NH_3 with AlH_3 molecule. The rate constant (k) of reaction via **tsba_AlN** is 1.30×10^{-1} s^{-1}. Although the rate constant from **tsba_AlN** is higher than those from **tsba_AlH_3** and **tsba_AlB**, the AlH_3 molecule cannot be put back into the system. From this reason, the AlH_3 molecule cannot serve as catalyst in the hydrogen elimination reactions of BH_3NH_3 with AlH_3. Furthermore, the equilibrium constants were calculated from equation (3.45) as shown in Table 4.1. The equilibrium constant (K) of the reaction via **tsba-AlH_3** of 1.85×10^{19} is obtained. It is found that the product **ba-ring-AlH_3** is more favorable product than the product BH_2NH_2 because its structure is more stable than the product BH_2NH_2.

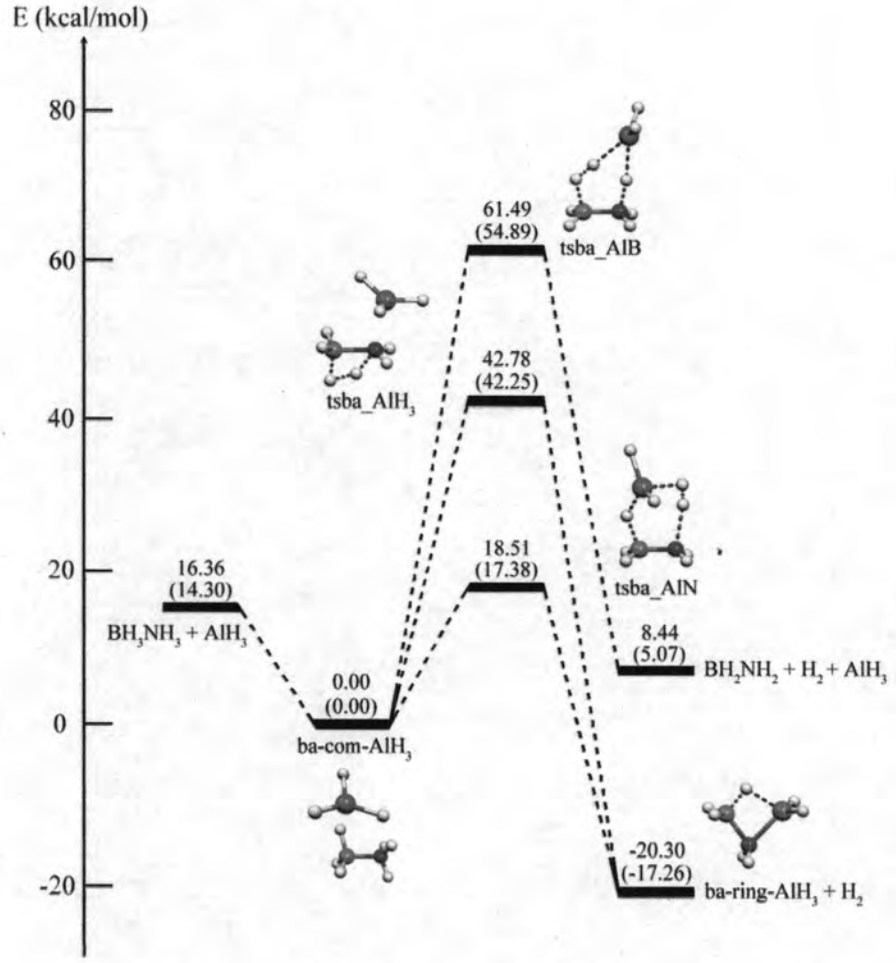

Figure 4.4 Reaction pathways for hydrogen release from BH_3NH_3 in the presence of AlH_3. Relative energies in kcal/mol computed at the MP2/6-311++G(d,p) and B3LYP/6-311++G(d,p) (in the parenthesis) levels of theory.

4.1.5 Reaction pathway for hydrogen release from BH_3NH_3 in the presence of PH_3

The schematic energy profile for hydrogen release from the borane amine with PH_3 is shown in Figure 4.5. Table 4.1 lists the relative energies calculated for hydrogen release from the BH_3NH_3 system computed at the MP2/6-311++G(d,p) and B3LYP/6-311++G(d,p) (in parenthesis). The initial energy interaction of BH_3NH_3 and PH_3 gives the **ba-com-PH_3**, which is 38.30 kcal/mol below the separated reactants BH_3NH_3 and PH_3. Starting from the **ba-com-PH_3**, three transition-state structures have been located, each representing a different type of hydrogen elimination are also shown in Figure A-5. The activation energies of three pathways in the second step via **tsba_PN**, **tsba_PH_3** and **tsba_PB** are 61.00, 45.83 and 38.25 kcal/mol, respectively.

The most favorable pathway is therefore the pathway via the transition state **tsba_PH$_3$**. However, the energy barrier via **tsba_PH$_3$** is higher than that found for the transition-state structure, **tsba**. As a result, the PH_3 molecule cannot play the role of a catalyst for hydrogen release from the borane amine with PH_3. Overall process gives the same separated products as BH_2NH_2, H_2 and PH_3. From all reaction energies via **tsba_PN**, **tsba_PH$_3$** and **tsba_PB** are negative that indicate over all reaction become exothermic processes.

For the hydrogen release via **tsba_PH$_3$**, we obtained $k = 1.30\times10^{-1}$ s^{-1}, this value include tunneling correction, see Table 4.1. In comparison with the rate constant of hydrogen release reaction via **tsba**, it is found that the rate constant is more than that via **tsba_PH$_3$**. In addition, the tunneling factors (κ) are listed in Table B-1, and the reaction constants are shown in Table 4.1.

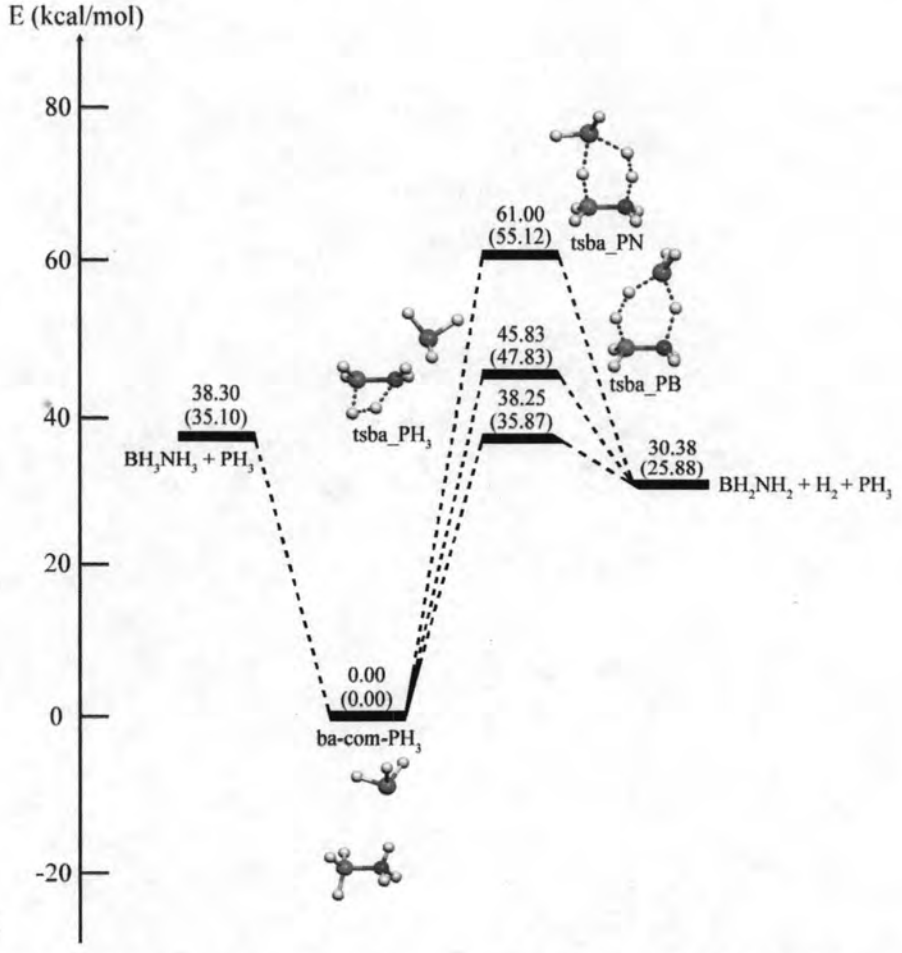

Figure 4.5 Reaction pathways for hydrogen release from BH_3NH_3 in the presence of PH_3. Relative energies in kcal/mol computed at the MP2/6-311++G(d,p) and B3LYP/6-311++G(d,p) (in the parenthesis) levels of theory.

The results show that the transition states **tsba_BN, tsba_NB** and **tsba_AlN** are stabilized by the BH_3, NH_3 and AlH_3, respectively and their structures are formed as the B···H···H···N, N···H···H···B and Al···H···H···N configurations respectively. The reason is that the strong electrostatic attraction between the positively charged H_N atom and the negatively charged H_B (or H_{Al}) atom. The **tsba_PH$_3$** is stabilized by the PH_3 as the most favorable transition state of which the structure of the four-membered framework is formed. This reason is that the PH_3 is the soft base [29] of which the hydrogen atom is not released. As the hydrogen release reaction via the transition state **tsba_AlN** affords the **ba-ring-AlH$_3$** which the AlH_3 is never released from its complex-state, therefore the AlH_3 is not a catalyst for this reaction process. For comparison with the experiment, the activation energy is 14.81 kcal/mol for the hydrogen release from BH_3NH_3 with the Co/γ-Al_2O_3 catalyst which is lower than the activation energy of 23.62 kcal/mol for the BH_3 catalyst from theoretical calculation.

4.2 Molecular mechanism of hydrogen release from AlH_3NH_3 system

Table 4.2 lists the relative energies, rate constants and thermodynamic properties calculated at the MP2/6-311++G(d,p) and B3LYP/6-311++G(d,p) (in the parenthesis) levels of theory for hydrogen release from the AlH_3NH_3 without and with the BH_3, NH_3, AlH_3 and PH_3. The reaction pathways for hydrogen release from AlH_3NH_3 system are illustrated in Figures 4.6-4.10.

4.2.1 Reaction pathway for synthesis of AlH_3NH_3 and hydrogen release from AlH_3NH_3

The corresponding energy profile for hydrogen release from the alane amine is shown in Figure 4.6. The relative energies, rate constants and thermodynamic properties of hydrogen release from the AlH_3NH_3 computed at the MP2/6-311++G(d,p) and B3LYP/6-311++G(d,p) (in parenthesis) are listed in Table 4.2. The reaction pathway for hydrogen release from BH_3NH_3 is composed of two reaction steps. The first step is the barrierless reaction, the spontaneous and exothermic reaction. The second step is the rate-determining step. The transition-state structure geometry, **tsala** for loss of hydrogen from the AlH_3NH_3 is similar to that for loss of

hydrogen from the BH_3NH_3. The shape and bond length for **tsala** is shown in Figure A-1(b). The energy barrier of the transition-state structure, **tsala** is calculated to be 29.53 kcal/mol. For hydrogen release from AlH_3NH_3, the AlH_3NH_3 monomer has a lower barrier than that found for BH_3NH_3 system. The reaction is endothermic by 2.88 kcal/mol.

We obtained the rate constants applying the TST and included a tunneling correction from equations (3.43) and (3.44). For hydrogen release from AlH_3NH_3, the rate constant (k) is 2.37×10^{-5} s^{-1} which is higher than that calculated for BH_3NH_3 system. Besides the equilibrium constants that calculated from equation (3.45) are listed in Table 4.2 and the tunneling factors (κ) are listed in Table B-2.

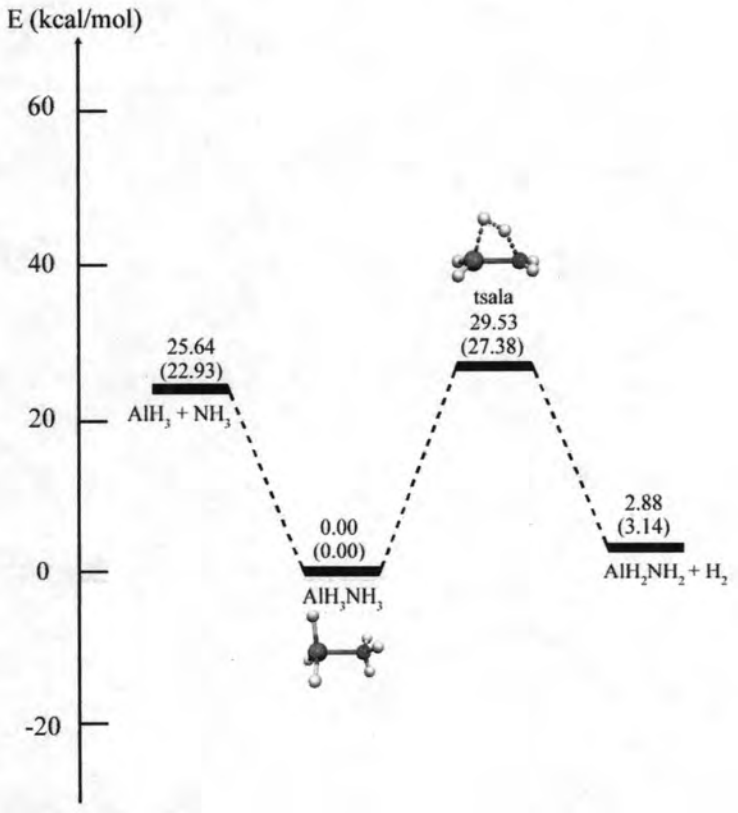

Figure 4.6 Reaction pathway for synthesis of AlH_3NH_3 and hydrogen release from AlH_3NH_3. Relative energies in kcal/mol computed at the MP2/6-311++G(d,p) and B3LYP/6-311++G(d,p) (in the parenthesis) levels of theory.

Table 4.2 Relative energies, rate constants and thermodynamic properties of hydrogen release from AlH_3NH_3 without and with BH_3, NH_3, AlH_3 or PH_3 catalyst, computed at the B3LYP/6-311++G(d,p) (in the parenthesis) and MP2/6-311++G(d,p) levels of theory

Reaction	$\Delta^{\ddagger}E^{a,b}$	k_{298} [c]	ΔE^{a}	ΔH_{298} [a]	ΔG_{298} [a]	K_{298}
AlH_3NH_3 reactant:						
$AlH_3+NH_3 \rightarrow AlH_3NH_3$	-	-	-25.64	-26.90	-17.57	7.54×10^{12}
	-	-	(-22.93)	(-24.15)	(-14.89)	(8.24×10^{10})
$AlH_3NH_3 \rightarrow$ **tsala** $\rightarrow AlH_2NH_2+H_2$	29.53	1.45×10^{-8}	2.88	4.47	-4.12	1.05×10^{3}
	(27.38)	(4.72×10^{-7})	(3.14)	(4.61)	(-3.76)	(5.74×10^{2})
AlH_3NH_3 and BH_3 reactants:						
$AlH_3NH_3+BH_3 \rightarrow AlH_3NH_3\cdots BH_3$	-	-	-31.87	-17.35	-8.05	3.71×10^{17}
	-	-	(-27.89)	(-14.97)	(-6.17)	(2.92×10^{14})
$AlH_3NH_3\cdots BH_3 \rightarrow$ **tsala-BN** $\rightarrow NH_2AlH_2BH_3$(ring)$+H_2$	45.85	1.92×10^{-21}	-37.12	-4.52	-10.61	6.04×10^{7}
	(40.13)	(3.40×10^{-17})	(-31.84)	(-3.16)	(-9.53)	(9.75×10^{6})
$AlH_3NH_3\cdots BH_3 \rightarrow$ **tsala-BH_3** $\rightarrow NH_2AlH_2BH_3+H_2$	29.74	7.32×10^{-10}	-31.30	2.15	-5.83	1.89×10^{4}
	(27.63)	(3.58×10^{-8})	(-27.32)	(2.02)	(-5.79)	(1.76×10^{4})
$AlH_3NH_3\cdots BH_3 \rightarrow$ **tsala-BAl** $\rightarrow AlH_2NH_2+H_2+BH_3$	85.27	3.23×10^{-50}	2.88	37.33	19.85	2.82×10^{-15}
	(75.83)	(3.45×10^{-43})	(3.14)	(33.57)	(15.97)	(1.97×10^{-12})
AlH_3NH_3 and NH_3 reactants:						
$AlH_3NH_3+NH_3 \rightarrow AlH_3NH_3\cdots NH_3$	-	-	-8.63	-9.02	-1.57	1.42×10^{1}
	-	-	(-7.45)	(-7.87)	(-0.36)	(1.83)
$AlH_3NH_3\cdots NH_3 \rightarrow$ **tsala-NN** $\rightarrow AlH_2NH_2+H_2+NH_3$	131.32	6.00×10^{-85}	2.88	13.49	-2.55	7.38×10^{1}
	(120.24)	(1.81×10^{-76})	(3.14)	(12.47)	(-3.41)	(3.14×10^{2})
$AlH_3NH_3\cdots NH_3 \rightarrow$ **tsala-NH_3** $\rightarrow AlH_2NH_2+H_2+NH_3$	33.63	1.10×10^{-11}	2.88	13.49	-2.55	7.38×10^{1}
	(31.43)	(8.85×10^{-10})	(3.14)	(12.47)	(-3.41)	(3.14×10^{2})
$AlH_3NH_3\cdots NH_3 \rightarrow$ **tsala-NAl** $\rightarrow AlH_2NH_2+H_2+NH_3$	24.52	6.87×10^{-7}	2.88	13.49	-2.55	7.38×10^{1}
	(24.04)	(1.21×10^{-6})	(3.14)	(12.47)	(-3.41)	(3.14×10^{2})
AlH_3NH_3 and AlH_3 reactants:						
$AlH_3NH_3+AlH_3 \rightarrow AlH_3NH_3\cdots AlH_3$	-	-	-20.86	-21.67	-12.39	1.20×10^{9}
	-	-	(-18.23)	(-18.97)	(-10.01)	(2.19×10^{7})
$AlH_3NH_3\cdots AlH_3 \rightarrow$ **tsala-AlN** $\rightarrow NH_2AlH_2AlH_3$(ring)$+H_2$	16.11	5.64	-39.45	-17.66	-24.17	5.23×10^{17}
	(10.37)	(6.18×10^{4})	(-34.10)	(-15.01)	(-21.17)	(3.33×10^{15})
$AlH_3NH_3\cdots AlH_3 \rightarrow$ **tsala-AlH_3** $\rightarrow NH_2AlH_2AlH_3+H_2$	29.85	8.61×10^{-10}	-22.87	-0.75	-8.28	1.17×10^{6}
	(28.34)	(5.39×10^{-9})	(-19.06)	(0.57)	(-6.98)	(1.30×10^{5})
$AlH_3NH_3\cdots AlH_3 \rightarrow$ **tsala-AlAl** $\rightarrow AlH_2NH_2+H_2+AlH_3$	70.30	8.91×10^{-39}	2.88	26.14	8.27	8.69×10^{-7}
	(61.70)	(1.09×10^{-32})	(3.14)	(23.57)	(6.25)	(2.62×10^{-5})
AlH_3NH_3 and PH_3 reactants:						
$AlH_3NH_3+PH_3 \rightarrow AlH_3NH_3\cdots PH_3$	-	-	-38.36	-38.16	-32.23	4.27×10^{23}
	-	-	(-33.57)	(-34.83)	(-30.27)	(1.54×10^{22})
$AlH_3NH_3\cdots PH_3 \rightarrow$ **tsala-PN** $\rightarrow AlH_2NH_2+H_2+PH_3$	63.01	4.01×10^{-35}	2.88	42.63	28.12	2.45×10^{-21}
	(56.75)	(4.17×10^{-32})	(3.14)	(39.44)	(26.50)	(3.71×10^{-20})
$AlH_3NH_3\cdots PH_3 \rightarrow$ **tsala-PH_3** $\rightarrow AlH_2NH_2+H_2+PH_3$	31.19	4.71×10^{-10}	2.88	42.63	28.12	2.45×10^{-21}
	(28.93)	(1.36×10^{-8})	(3.14)	(39.44)	(26.50)	(3.71×10^{-20})
$AlH_3NH_3\cdots PH_3 \rightarrow$ **tsala-PAl** $\rightarrow AlH_2NH_2+H_2+PH_3$	46.04	4.61×10^{-23}	2.88	42.63	28.12	2.45×10^{-21}
	(35.24)	(9.50×10^{-16})	(3.14)	(39.44)	(26.50)	(3.71×10^{-20})

[a] In kcal/mol.
[b] Activation energy.
[c] In s^{-1}

4.2.2 Reaction pathway for hydrogen release from AlH_3NH_3 in the presence of BH_3

This pathway is also relevant to hydrogen production in that decomposition of AlH_3NH_3 is now assisted by borane. The geometries for this set of reaction paths are given in Figure A-6, and the energy profile for hydrogen release from the alane amine with borane is shown in Figure 4.7. Their relative energies, rate constants and thermodynamic properties of hydrogen release from AlH_3NH_3 with BH_3 computed at the MP2/6-311++G(d,p) and B3LYP/6-311++G(d,p) (in the parenthesis) are listed in Table 4.2. The reaction pathways for hydrogen release from AlH_3NH_3 in presence with BH_3 are composed of two reaction steps. The first step is the barrierless reaction, the complex **ala-com-BH_3** is stable relative to the reactants by 31.87 kcal/mol. The second step, the three transition-state structures have been located via **tsala_BN**, **tsala_BH_3** and **tsala_BAl** as shown in Figure A-6. Normal mode for the imaginary frequencies of **tsala_BN**, **tsala_BH_3** and **tsala_BB** are shown in Table B-2. In transition-state structures, **tsala_BN**, the energy barrier is calculated to be 45.85 kcal/mol. It is of interest that the product of this process is the three membered-ring resulting the **ala-ring-BH_3**, which the BH_3 is never released from its complex-state. Therefore, the BH_3 cannot act as the catalyst. The rate constants of this reaction can be evaluated by equations (3.43) and (3.44), $k = 1.92\times10^{-21}$ s^{-1}.

For **tsala_BH_3**, the transition state corresponds to **tsba_BH_3** described above. The energy barrier involving **tsala_BH_3** is calculated to be 29.74 kcal/mol. The process via **tsala_BH_3** proceeds with lowest energy, however, the product of this process is the complex $NH_2AlH_2BH_3$ which is not AlH_2NH_2, H_2 and BH_3 then the BH_3 molecule cannot serve as a catalyst in this process. The transition state **tsala_BAl**, the shape and characteristics are similar in **tsba_BB** discussed above. The energy barrier of transition state, **tsala_BAl** is calculated to be 85.27 kcal/mol. The transition state, **tsala_BAl** is far more stable than **tsala_BH_3**, with energy difference of 55.53 kcal/mol.

In addition, the tunneling factors (κ) and rate constants of all hydrogen release compound systems are listed in Tables B-2 and 4.2, respectively. The equilibrium constants (K) calculated from equation (3.45) of the reaction via **tsala_BH_3** and **tsala_BN** are 1.89×10^{4} and 6.04×10^{7}, respectively. It was found that the product

ala-ring-BH_3 is more favorable product than the product $NH_2AlH_2BH_3$ because its structure is more stable than the product $NH_2AlH_2BH_3$.

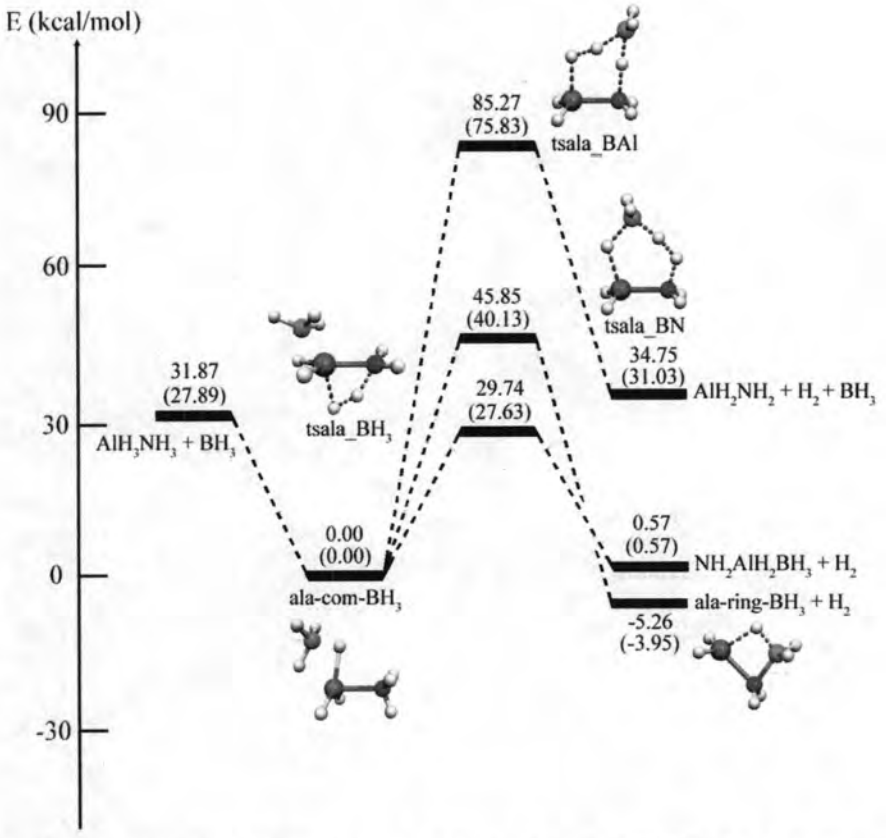

Figure 4.7 Reaction pathways for hydrogen release from AlH_3NH_3 in the presence of BH_3. Relative energies in kcal/mol computed at the MP2/6-311++G(d,p) and B3LYP/6-311++G(d,p) (in the parenthesis) levels of theory.

4.2.3 Reaction pathway for hydrogen release from AlH_3NH_3 in the presence of NH_3

The corresponding energy profile is illustrated in Figure 4.8 and Table 4.2 lists their relative energies, rate constants and thermodynamic properties of hydrogen release from AlH_3NH_3 in the presence of NH_3. For the AlH_3NH_3 + NH_3 reaction, we located three different transition-state structures such as the BH_3NH_3 +NH_3 reaction. The shape and characteristics of the stationary points involving NH_3 are similar in many respects to those involving BH_3 discussed above. The first step, the complex **ala-com-NH_3** between AlH_3NH_3 and NH_3 is formed which of the reaction energy is 8.63 kcal/mol. The second step is composed of three transition-state structures via **tsala_NN**, **tsala_NH_3** and **tsala_NAl** as shown in Figure A-7. The transition state

tsala_NH$_3$ corresponds to **tsala_BH$_3$** described above, in which NH_3 now interacts with **tsala** of the monomer from outside of the four-membered ring and by H-bonding. Calculate the energy barrier involving **tsala_NH$_3$** is 33.63 kcal/mol. The process via **tsala_NN** and **tsala_NAl**, the transition-state structures are similar in the process via **tsala_BN** and **tsala_BAl**, respectively. The transition-state structure, **tsala_NAl** is the lowest energy transition structure, with an energy barrier of 15.89 kcal/mol relative to the separated reactants, which represents a reduction of 13.64 kcal/mol with respect to the energy barrier of 29.53 kcal/mol in the AlH_3NH_3 monomer via **tsala** in system without the NH_3.

Furthermore, the rate constants of the catalytic processes, we can evaluate by equations (3.43) and (3.44). The rate constants (k) via **tsala_NN**, **tsala_NH$_3$** and **tsala_NAl** are 6.00×10^{-85}, 1.10×10^{-11} and 6.87×10^{-7} s^{-1}, respectively. From these values show that the transfer of two H-atoms from AlH_3NH_3 should be significantly faster in transition-state structures, **tsala_NAl** than in **tsala_NN** and **tsala_NH$_3$**. The tunneling factors (κ) and equilibrium constants (K) are listed in Tables B-2 and 4.2, respectively.

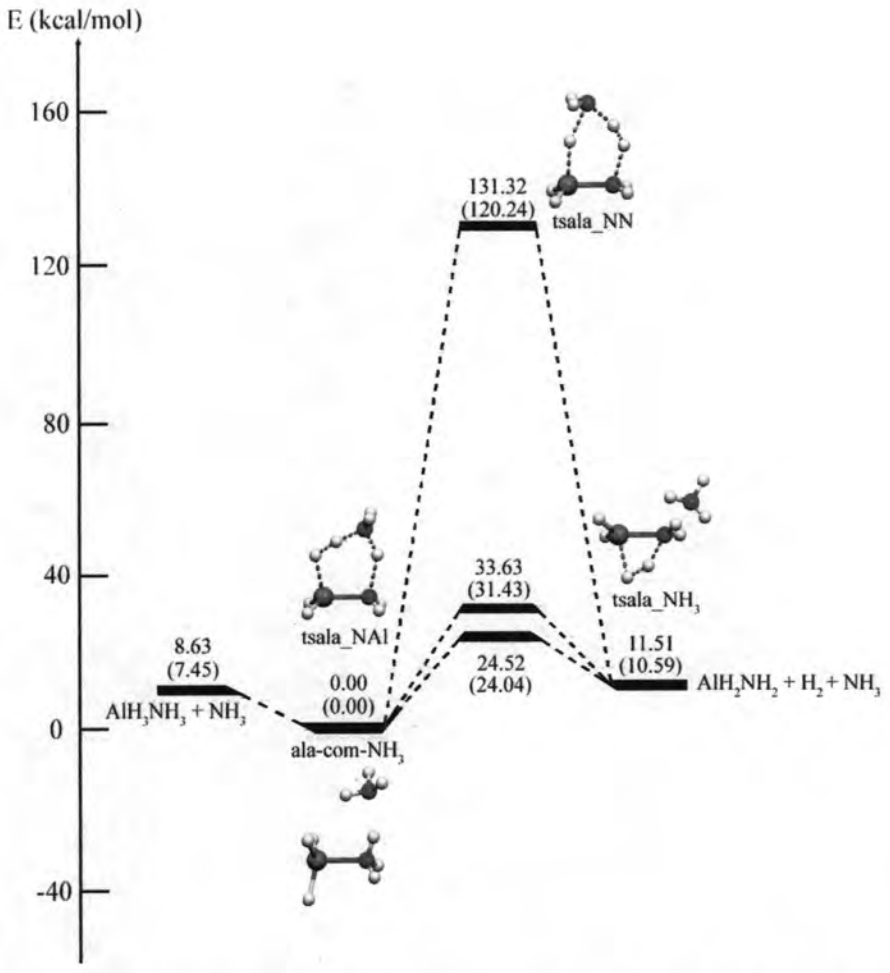

Figure 4.8 Reaction pathways for hydrogen release from AlH_3NH_3 in the presence of NH_3. Relative energies in kcal/mol computed at the MP2/6-311++G(d,p) and B3LYP/6-311++G(d,p) (in the parenthesis) levels of theory.

4.2.4 Reaction pathway for hydrogen release from AlH_3NH_3 in the presence of AlH_3

For the AlH_3NH_3 + AlH_3 reaction, we located a complex and three transition-state structures are displayed in Figure A-8. The corresponding energy profile for hydrogen release from the alane amine with the presence of AlH_3 is illustrated in Figure 4.9. Table 4.2 lists the relative energies, rate constants and thermodynamic properties calculated at the MP2/6-311++G(d,p) and B3LYP/6-311++G(d,p) (in the parenthesis). The reaction pathways for hydrogen release from AlH_3NH_3 with AlH_3 are composed of two reaction steps. Starting from **ala-com-AlH_3**, three transition state structures have been located, each representing a different type of hydrogen elimination. The transition-state structures, **tsala_AlN**, **tsala_AlH_3** and **tsala_AlAl**

are illustrated in Figure A-8. The activation energies of three pathways in the second step via **tsala_AlN**, **tsala_AlH$_3$** and **tsala_AlAl** are 16.11, 29.85 and 70.30 kcal/mol, respectively. The least favorable pathway is therefore the pathway via the transition-state structure, **tsala_AlH$_3$**. The product from this process is aminodialane $NH_2AlH_2AlH_3$, which of the reaction energies are 22.88 kcal/mol below the reactants.

In the transition state **tsala_AlN**, the energy barrier is calculated to be 16.11 kcal/mol. The process via **tsala_AlN** is lowest energy. This pathway results the three-membered ring, **ala-ring-AlH$_3$** which the AlH_3 is never released from its complex-state. Therefore, the AlH_3 molecule cannot act as a catalyst via this process because the AlH_3 molecule cannot be put back into the system.

Table 4.2 lists the calculated rate constants, including tunneling corrections, using TST for each process in this system from equations (3.43) and (3.44). Table B-2 shows the tunneling factors (κ) for all hydrogen storage compound systems. Furthermore, the equilibrium constants calculated are shown in Table 4.2. The equilibrium constants were calculated from equation (3.45) which the equilibrium constant (K) via **tsala-AlN** is 5.23×10^{17}. It is found that the product **ala-ring-AlH$_3$** is more favorable product than the product AlH_2NH_2 because its structure is more stable than the product AlH_2NH_2.

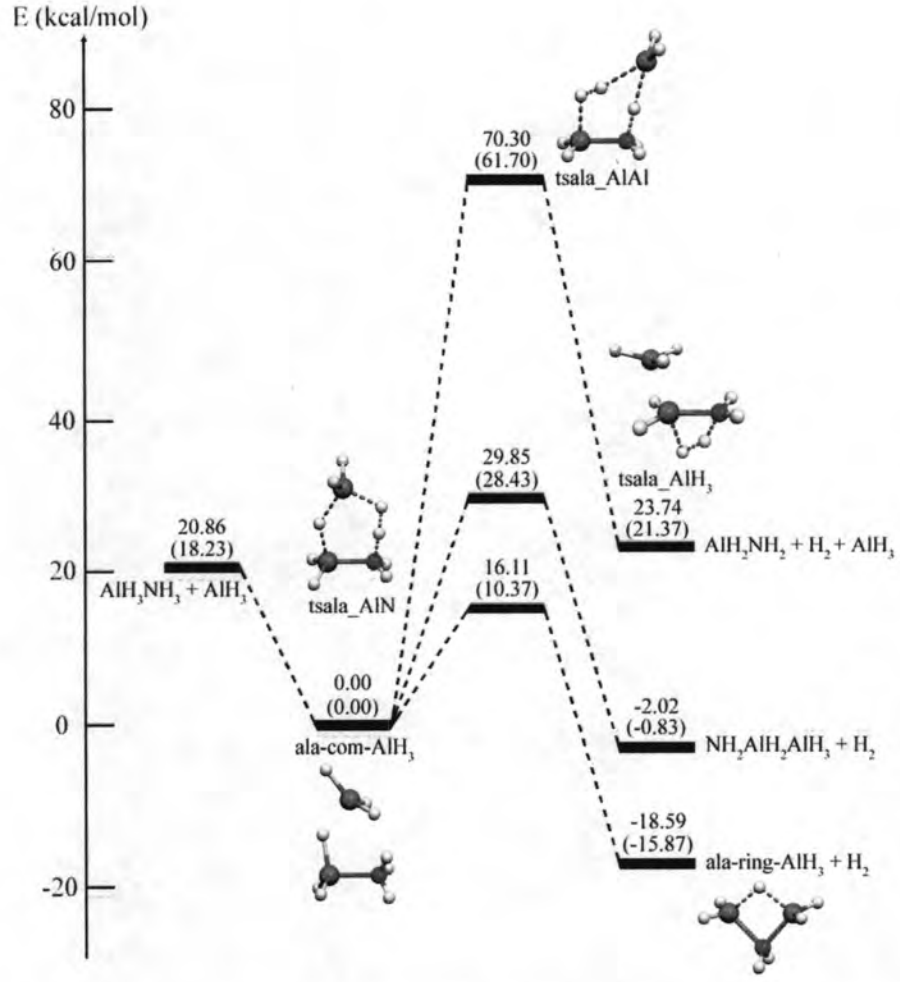

Figure 4.9 Reaction pathways for hydrogen release from AlH_3NH_3 in the presence of AlH_3. Relative energies in kcal/mol computed at the MP2/6-311++G(d,p) and B3LYP/6-311++G(d,p) (in the parenthesis) levels of theory.

4.2.5 Reaction pathway for hydrogen release from AlH_3NH_3 in the presence of PH_3

We have considered the hydrogen release mechanism from AlH_3NH_3 involving an additional phosphine molecule. Table 4.2 lists their relative energies, rate constants and thermodynamic properties of hydrogen release from AlH_3NH_3 in the presence of PH_3 and the corresponding energy profile is illustrated in Figure 4.10. The reaction pathways for hydrogen release from AlH_3NH_3 with PH_3 are composed of two reaction steps. The first step is the barrierless reaction which the complex **ala-com-PH_3** is formed. The second step, the three transition-state structures have been located via **tsala_PN**, **tsala_PH_3** and **tsala_PAl** as shown in Figure A-9. Normal modes for the imaginary frequencies of three transition states are listed in Table B-2.

The energies barrier via **tsala_PN** and **tsala_PAl** are 63.01 and 46.04 kcal/mol, respectively. The **tsala_PH_3** corresponds to **tsala_NH_3** described above which the energy barrier involving **tsala_PH_3** is calculated to be 31.19 kcal/mol. The transition-state structure, **tsala_PH_3** is the lowest energy transition structure. Nevertheless, the energy barrier via **tsala_ PH_3** is higher than that found for **tsala** in system without any catalyst. As a result, the PH_3 molecule cannot play the role of a catalyst for hydrogen release from alane amine with PH_3. Overall process gives the same separated products as AlH_2NH_2, H_2 and PH_3. From all reaction energies via **tsala_PN**, **tsala_PH_3** and **tsala_PAl** are positive that indicate over all reaction become endothermic processes by 2.88 kcal/mol with respect the reactants.

The rate constants of these processes, we can evaluate by equations (3.43) and (3.44). The rate constants (k) via **tsala_PN**, **tsala_PH_3** and **tsala_PAl** are 4.01×10^{-35}, 4.71×10^{-10} and 4.61×10^{-23} s^{-1}, respectively. From these values show that the transfer of two H-atoms from AlH_3NH_3 should be significantly faster in the transition-state structure, **tsala_PH_3** than in **tsala_PN** and **tsala_PAl**. In addition, the tunneling factors (κ) and equilibrium constants (K) are listed in Tables B-2 and 4.2, respectively.

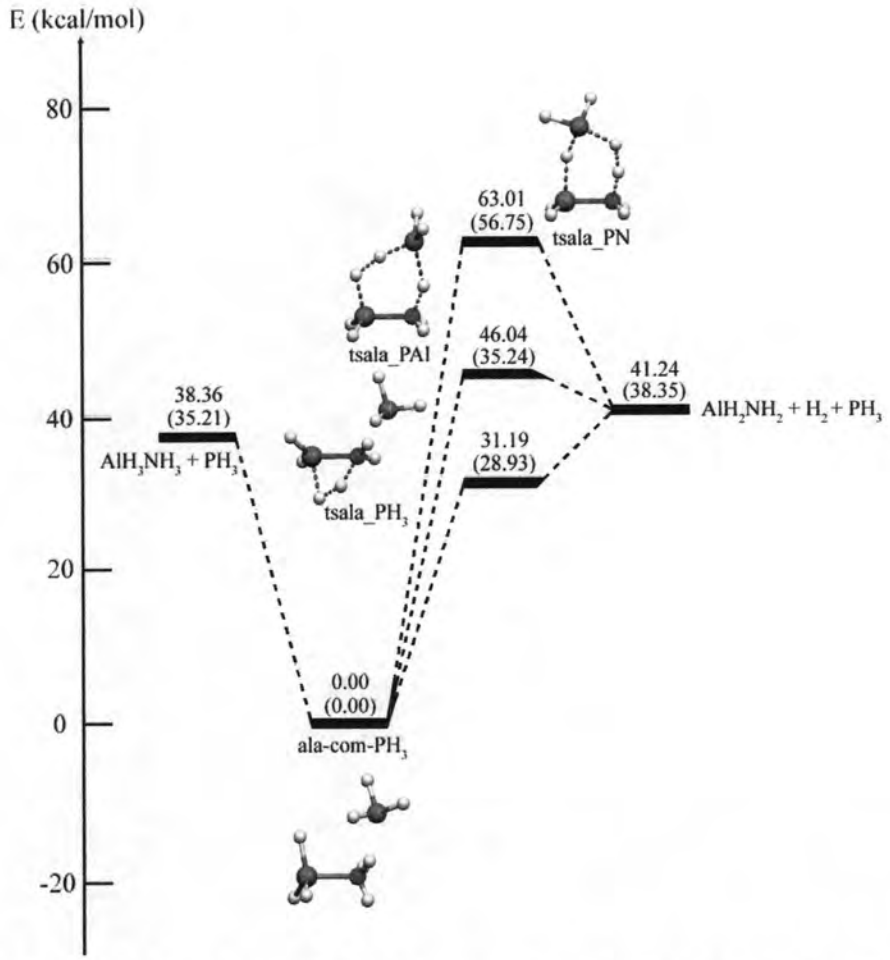

Figure 4.10 Reaction pathways for hydrogen release from AlH_3NH_3 in the presence of PH_3. Relative energies in kcal/mol computed at the MP2/6-311++G(d,p) and B3LYP/6-311++G(d,p) (in the parenthesis) levels of theory.

The results show that the transition states **tsala_NAl** and **tsala_AlN** are stabilized by the NH_3 and AlH_3, respectively and their structures are formed as the N···H···H···Al, and Al···H···H···N configurations respectively. The reason is that the strong electrostatic attraction between the positively charged H_N atom and the negatively charged H_{Al} atom. The **tsala_PH$_3$** is stabilized by the PH_3 as the most favorable transition state of which the structure of the four-membered framework is formed. This reason is that the PH_3 is the soft base of which the hydrogen atom is not released. As the hydrogen release reaction via the transition states, **tsala_BH$_3$** and **tsala_AlN** afford the complex $NH_2AlH_2BH_3$ and **ba-ring-AlH$_3$**, respectively which the BH_3 and AlH_3 molecules cannot be released as the free species, therefore these reaction pathways is not considered as the catalytic reactions.

4.3 Molecular mechanism of hydrogen release from BH_3PH_3 system

Table 4.3 lists the relative energies, rate constants and thermodynamic properties calculated at the MP2/6-311++G(d,p) and B3LYP/6-311++G(d,p) (in the parenthesis) levels of theory for hydrogen release from BH_3PH_3 without and with the BH_3, NH_3, AlH_3 and PH_3. The reaction pathways for hydrogen release from BH_3PH_3 system are shown in Figures 4.11-4.15.

4.3.1 Reaction pathway for synthesis of BH_3PH_3 and hydrogen release from BH_3PH_3

The calculated results for the decomposition of borane phosphine are summarized in Figure 4.11 and Figure A-1(c). The relative energies, rate constants and thermodynamic properties of hydrogen release from BH_3PH_3 computed at the MP2/6-311++G(d,p) and B3LYP/6-311++G(d,p) (in the parenthesis) levels of theory are listed in Table 4.3. The reaction pathway for hydrogen release from BH_3PH_3 is composed of two reaction steps. The first step is the barrierless reaction and exothermic reaction. The second step is the rate-determining step. The transition-state structure geometry, **tsbp** for loss of hydrogen from BH_3PH_3 is similar to that for loss of hydrogen from BH_3NH_3 and AlH_3NH_3. The H–H distance of 1.24 Å, see Figure A-1(c) is substantially longer than that of 0.99 Å in the transition state structure of borane amine. The energy barrier of the transition-state structure, **tsbp** was calculated to be 47.42 kcal/mol.

We performed the rate constants using the TST and included a tunneling correction from equations (3.43) and (3.44). For hydrogen release from BH_3PH_3, the rate constant is $k = 5.01\times10^{-21}$ s^{-1} which is lower than that calculated for BH_3NH_3 system. Moreover the equilibrium constants that calculated from equation (3.45) and the tunneling factors (κ) are list in Tables 4.3 and B-3, respectively.

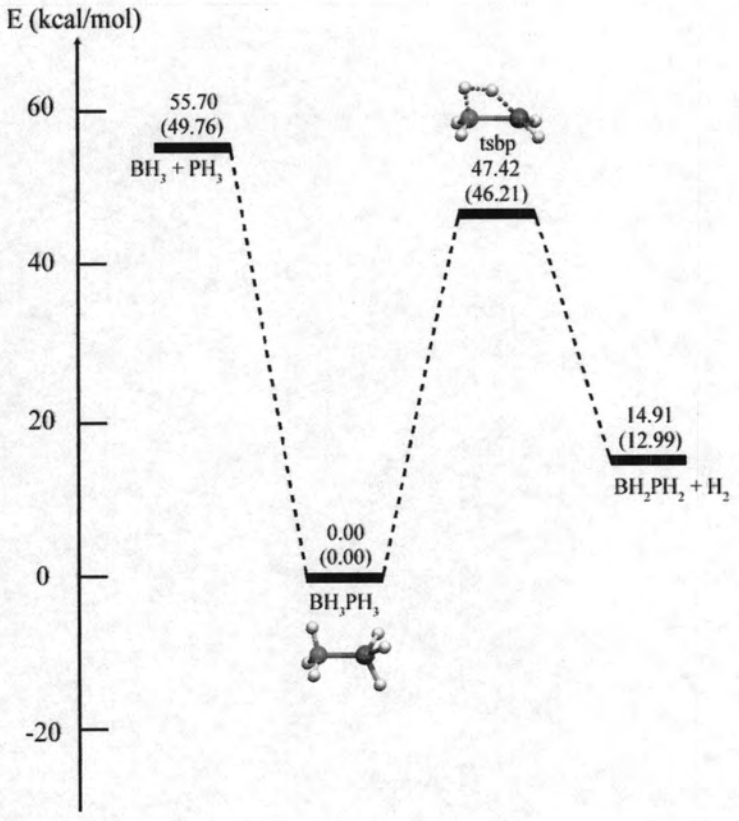

Figure 4.11 Reaction pathway for synthesis of BH_3PH_3 and hydrogen release from BH_3PH_3. Relative energies in kcal/mol computed at the MP2/6-311++G(d,p) and B3LYP/6-311++G(d,p) (in the parenthesis) levels of theory.

Table 4.3 Relative energies, rate constants and thermodynamic properties of hydrogen release from BH_3PH_3 without and with BH_3, NH_3, AlH_3 or PH_3 catalyst, computed at the B3LYP/6-311++G(d,p) (in the parenthesis) and MP2/6-311++G(d,p) levels of theory

Reaction	$\Delta^{\ddagger}E^{a,b}$	$k_{298}{}^{c}$	ΔE^{a}	$\Delta H_{298}{}^{a}$	$\Delta G_{298}{}^{a}$	K_{298}
BH_3PH_3 reactant:						
$BH_3+PH_3 \rightarrow BH_3PH_3$	-	-	-55.70	-57.17	-47.67	8.88×10^{34}
	-	-	(-49.76)	(-51.17)	(-41.78)	(4.24×10^{30})
$BH_3PH_3 \rightarrow$ **tsbp** $\rightarrow BH_2PH_2+H_2$	47.42	5.01×10^{-21}	14.91	16.59	7.59	2.73×10^{-6}
	(46.21)	(2.66×10^{-20})	(12.99)	(14.63)	(5.71)	(6.54×10^{-5})
BH_3PH_3 and BH_3 reactants:						
$BH_3PH_3+BH_3 \rightarrow BH_3PH_3\cdots BH_3$	-	-	-10.77	-12.03	-2.34	5.17×10^{1}
	-	-	(-7.32)	(-8.42)	(0.86)	(2.33×10^{-1})
$BH_3PH_3\cdots BH_3 \rightarrow$ **tsbp-BP** $\rightarrow PH_2BH_2BH_3$(ring)$+H_2$	31.13	1.08×10^{-10}	-19.78	-7.83	-14.71	6.03×10^{10}
	(27.36)	(3.99×10^{-8})	(-12.89)	(-4.52)	(-11.03)	(1.22×10^{8})
$BH_3PH_3\cdots BH_3 \rightarrow$ **tsbp-BH_3** $\rightarrow PH_2BH_2BH_3+H_2$	21.45	2.29×10^{-3}	-2.60	10.11	0.99	1.89×10^{-1}
	(18.91)	(9.89×10^{-2})	(-0.39)	(8.70)	(0.03)	(9.50×10^{-1})
$BH_3PH_3\cdots BH_3 \rightarrow$ **tsbp-BB** $\rightarrow BH_2PH_2+H_2+BH_3$	61.12	6.01×10^{-32}	14.91	28.62	9.93	5.27×10^{-8}
	(56.23)	(2.24×10^{-28})	(12.99)	(23.05)	(4.85)	(2.80×10^{-4})
BH_3PH_3 and NH_3 reactants:						
$BH_3PH_3+NH_3 \rightarrow BH_3PH_3\cdots NH_3$	-	-	-3.87	-3.79	2.40	1.73×10^{-2}
	-	-	(-2.29)	(-2.03)	(2.53)	(1.39×10^{-2})
$BH_3PH_3\cdots NH_3 \rightarrow$ **tsbp-NP** $\rightarrow BH_2PH_2+H_2+NH_3$	83.61	1.79×10^{-50}	14.91	20.38	5.19	1.57×10^{-4}
	(78.07)	(9.82×10^{-48})	(12.99)	(16.66)	(3.18)	(4.70×10^{-3})
$BH_3PH_3\cdots NH_3 \rightarrow$ **tsbp-NH_3** $\rightarrow BH_2PH_2+H_2+NH_3$	60.48	1.35×10^{-32}	14.91	20.38	5.19	1.57×10^{-4}
	(57.26)	(1.12×10^{-30})	(12.99)	(16.66)	(3.18)	(4.70×10^{-3})
$BH_3PH_3\cdots NH_3 \rightarrow$ **tsbp-NB** $\rightarrow PH_2BH_2NH_3+H_2$	41.21	1.16×10^{-19}	-8.95	-4.96	-9.28	6.32×10^{6}
	(46.65)	(1.26×10^{-24})	(-5.40)	(-5.19)	(-5.88)	(2.06×10^{4})
BH_3PH_3 and AlH_3 reactants:						
$BH_3PH_3+AlH_3 \rightarrow BH_3NH_3\cdots AlH_3$	-	-	-11.16	-11.75	-3.26	2.46×10^{2}
	-	-	(-7.90)	(-8.39)	(-0.28)	(1.60)
$BH_3PH_3\cdots AlH_3 \rightarrow$ **tsbp-AlP** $\rightarrow PH_2BH_2AlH_3$(ring)$+H_2$	21.34	4.39×10^{-4}	-20.03	-7.71	-14.52	4.40×10^{10}
	(18.14)	(1.04×10^{-1})	(-15.46)	(-6.49)	(-12.94)	(3.08×10^{9})
$BH_3PH_3\cdots AlH_3 \rightarrow$ **tsbp-AlH_3** $\rightarrow BH_2PH_2+H_2+AlH_3$	29.26	4.17×10^{-9}	14.91	28.34	10.85	1.11×10^{-8}
	(25.16)	(2.83×10^{-6})	(12.99)	(23.01)	(5.98)	(4.10×10^{-5})
$BH_3PH_3\cdots AlH_3 \rightarrow$ **tsbp-AlB** $\rightarrow BH_2PH_2+H_2+AlH_3$	60.14	3.29×10^{-32}	14.91	28.34	10.85	1.11×10^{-8}
	(52.21)	(2.52×10^{-26})	(12.99)	(23.01)	(5.98)	(4.10×10^{-5})
BH_3PH_3 and PH_3 reactants:						
$BH_3PH_3+PH_3 \rightarrow BH_3NH_3\cdots PH_3$	-	-	-36.52	-36.11	-30.97	5.02×10^{22}
	-	-	(-33.47)	(-32.74)	(-30.25)	(1.50×10^{22})
$BH_3PH_3\cdots PH_3 \rightarrow$ **tsbp-PP** $\rightarrow BH_2PH_2+H_2+PH_3$	66.61	8.32×10^{-39}	14.91	52.70	38.56	5.44×10^{-29}
	(60.80)	(2.78×10^{-36})	(12.99)	(47.36)	(35.96)	(4.36×10^{-27})
$BH_3PH_3\cdots PH_3 \rightarrow$ **tsbp-PH_3** $\rightarrow BH_2PH_2+H_2+PH_3$	52.45	2.82×10^{-26}	14.91	52.70	38.56	5.44×10^{-29}
	(44.82)	(6.87×10^{-21})	(12.99)	(47.36)	(35.96)	(4.36×10^{-27})
$BH_3PH_3\cdots PH_3 \rightarrow$ **tsbp-PB** $\rightarrow BH_2PH_2+H_2+PH_3$	57.59	1.71×10^{-31}	14.91	52.70	38.56	5.44×10^{-29}
	(51.72)	(3.56×10^{-29})	(12.99)	(47.36)	(35.96)	(4.36×10^{-27})

[a] In kcal/mol.
[b] Activation energy.
[c] In s^{-1}

4.3.2 Reaction pathway for hydrogen release from BH_3PH_3 in the presence of BH_3

Table 4.3 lists the relative energies calculated at the MP2/6-311++G(d,p) and B3LYP/6-311++G(d,p) (in parenthesis) levels of theory for hydrogen release from BH_3PH_3 in the presence of BH_3. The first step is the complexation of BH_3PH_3 and BH_3 resulting the **bp-com-BH_3**, this step is the barrierless and its reaction is the spontaneous and exothermic process. The second step, from complex, **bp-com-BH_3**, three transition state structures have been located, each representing a different type of hydrogen elimination are also shown in Figure A-10. The transition-state structure, **tsbp-BH_3** corresponds to a process in which the BH_3 interacts with the **tsbp** of the BH_3PH_3 monomer. For the transition states via **tsbp_BB** and **tsbp_BP**, the energies barrier are 61.12 and 31.13 kcal/mol, respectively. The product via **tsbp_BP** is the three membered-ring resulting the **bp-ring-BH_3**. The energy barrier via transition state, **tsbp-BH_3** of 21.45 kcal/mol is found. The product of this process is the complex, $PH_2BH_2BH_3$. Thus, the most favorable pathway is therefore the pathway via the transition-state structure, **tsbp_BH_3**. The activation energy of the most favorable path, via the **tsbp_BH_3** is lower than its corresponding hydrogen storage compound in system without BH_3 by 15.97 kcal/mol. Because the BH_3 molecule cannot be put back into the system, the BH_3 molecule cannot act as a catalyst via this process.

In addition, the tunneling factors (κ) and rate constants are listed in Tables B-3 and 4.3, respectively. The equilibrium constants can be calculated by equation (3.45) as shown in Table 4.3. For the transition-state structures, **tsbp_BH_3** and **tsbp_BP**, the equilibrium constants (K) are 1.89×10^{-1} and 6.03×10^{10}, respectively. It is found that the product **bp-ring-BH_3** is more favorable product than the product $PH_2BH_2BH_3$ because its structure is more stable than the product $PH_2BH_2BH_3$.

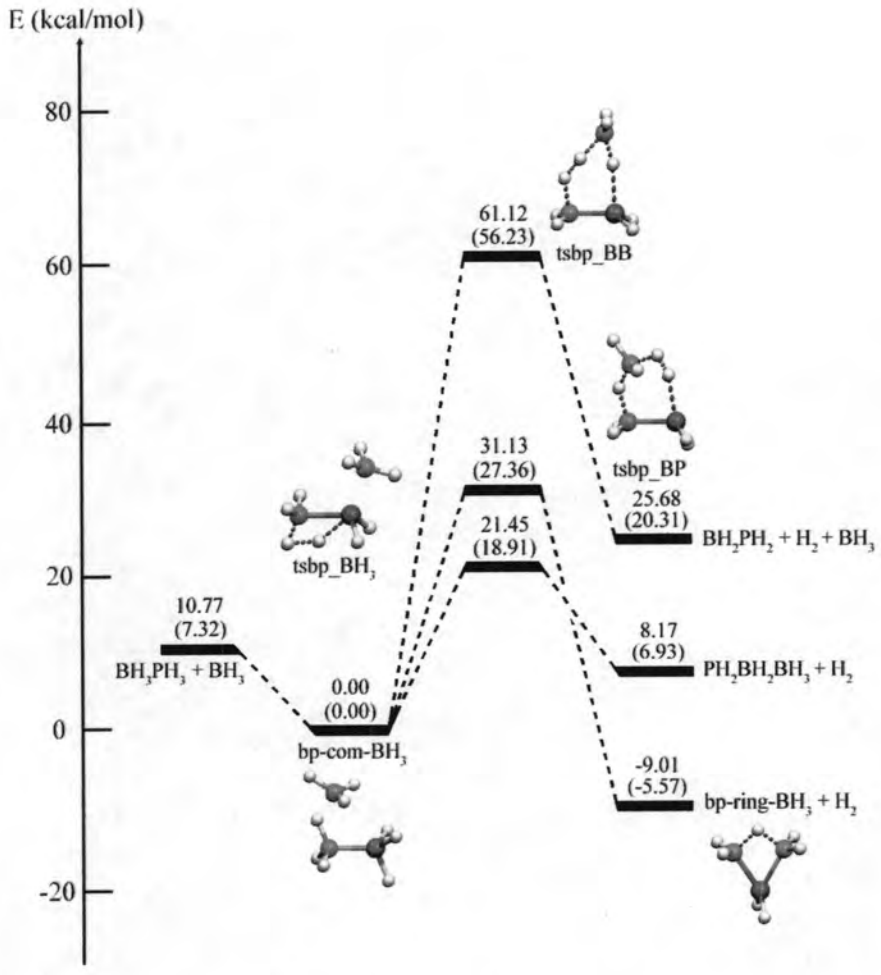

Figure 4.12 Reaction pathways for hydrogen release from BH_3PH_3 in the presence of BH_3. Relative energies in kcal/mol computed at the MP2/6-311++G(d,p) and B3LYP/6-311++G(d,p) (in the parenthesis) levels of theory.

4.3.3 Reaction pathway for hydrogen release from BH_3PH_3 in the presence of NH_3

The relative energies, rate constants and thermodynamic properties of hydrogen release from BH_3PH_3 with NH_3 system computed at the MP2/6-311++G(d,p) and B3LYP/6-311++G(d,p) (in the parenthesis) levels of theory are listed in Table 4.3. The reaction pathways for hydrogen release from BH_3PH_3 with NH_3 molecule are composed of two reaction steps as shown in Figure 4.13. The first step is the barrierless reaction and exothermic process. The complexation energy of **bp-com-NH_3** is 3.87 kcal/mol with respect from the reactants. The second step, the transition-state structures have been located and the energy profile is given in

Figure 4.13. The transition-state structures have been located via **tsbp_NB**, **tsbp_NH$_3$** and **tsbp_NP** as shown in Figure A-11. The activation energies of three pathways in the second step via **tsbp_NB**, **tsbp_NH$_3$** and **tsbp_NP** are 41.21, 60.48 and 83.61 kcal/mol, respectively. Based on the NH_3 catalytic reaction, for hydrogen release from BH_3PH_3, the most favorable pathway for this hydrogen release process is therefore the reaction via transition state **tsbp_NH$_3$** and affords the products BH_2PH_2, H_2 and NH_3 catalyst. Even though, the activation energy due to the transition state **tsbp_NB** is the lowest energy, the NH_3 molecule cannot be released as the free species but formed as the complex $PH_2BH_2NH_3$. As the NH_3 does not behave as the catalyst, this reaction pathway is not considered as the hydrogen energy resource.

In addition, the tunneling factors (κ) and rate constants are listed in Tables B-3 and 4.3, respectively. The equilibrium constants can be calculated by equation (3.45) as shown in Table 4.3. For the hydrogen release reaction via **tsbp_NB** and **tsbp_NP**, the equilibrium constants (K) are 6.32×10^{6} and 1.57×10^{-4}, respectively. It is found that the product $PH_2BH_2NH_3$ is more favorable product than the product BH_2PH_2 because it is more stable than the product BH_2PH_2.

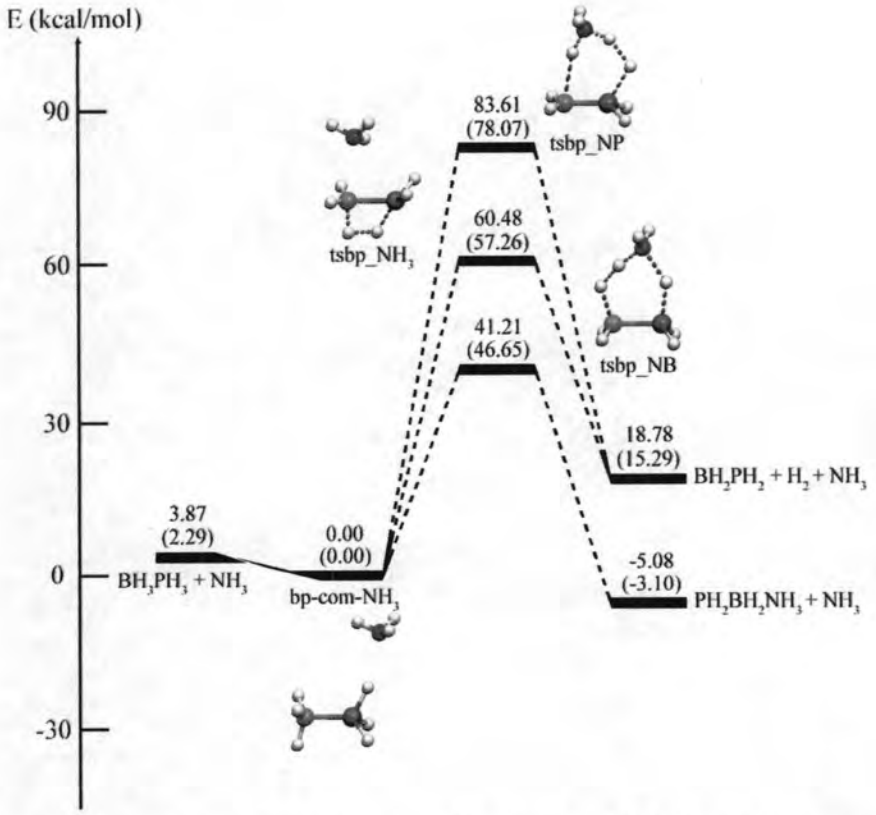

Figure 4.13 Reaction pathways for hydrogen release from BH_3PH_3 in the presence of NH_3. Relative energies in kcal/mol computed at the MP2/6-311++G(d,p) and B3LYP/6-311++G(d,p) (in the parenthesis) levels of theory.

4.3.4 Reaction pathway for hydrogen release from BH_3PH_3 in the presence of AlH_3

The corresponding energy profile is illustrated in Figure 4.14 and Table 4.3 lists the relative energies, rate constants and thermodynamic properties of hydrogen release from BH_3PH_3 in the presence of AlH_3. For the BH_3PH_3 + AlH_3 reaction, we located three different transition-state structures such as the BH_3NH_3 +AlH_3 reaction. The shape and characteristics of the stationary points involving AlH_3 are similar in many respects to those involving BH_3 discussed above. The first step, the complex **bp-com-AlH_3** between BH_3PH_3 and AlH_3 is formed. The second step is composed of three transition-state structures via **tsbp_AlP**, **tsbp_AlH_3** and **tsbp_AlB** as shown in Figure A-12. The activation energies of three pathways in the second step via **tsbp_AlP**, **tsbp_AlH_3** and **tsbp_AlB** are 21.34, 29.26 and 60.14 kcal/mol, respectively. In transition states, **tsbp_AlH_3** and **tsbp_AlB** result the same separated products as BH_2PH_2, H_2 and AlH_3. Although the hydrogen release from BH_3PH_3 with

the AlH_3 via **tsbp_AlP** is the lowest energy, the AlH_3 molecule cannot be released from the complex-state but formed as the **bp-ring-AlH_3**. Therefore, the AlH_3 does not behave as the catalyst for hydrogen release via the transition state **tsbp_AlP**. The second most favorable pathway is therefore the pathway via the transition state **tsbp_AlH_3** shows that the AlH_3 molecule can serve as a catalyst for hydrogen release from borane phosphine with AlH_3.

The rate constants of these processes, we can evaluate by equations (3.43) and (3.44). The rate constants (k) via **tsbp_AlP**, **tsbp_AlH_3** and **tsbp_AlB** are 4.39×10^{-4}, 4.17×10^{-9} and 3.29×10^{-32} s^{-1}, respectively. The rate constants calculated show that the hydrogen release reaction from BH_3PH_3 with the AlH_3 via **tsbp_AlP** is faster than that via **tsbp_AlH_3** and **tsbp_AlB**. In addition, the tunneling factors (κ) and the equilibrium constants from equation (3.45) are listed in Tables B-3 and 4.3, respectively.

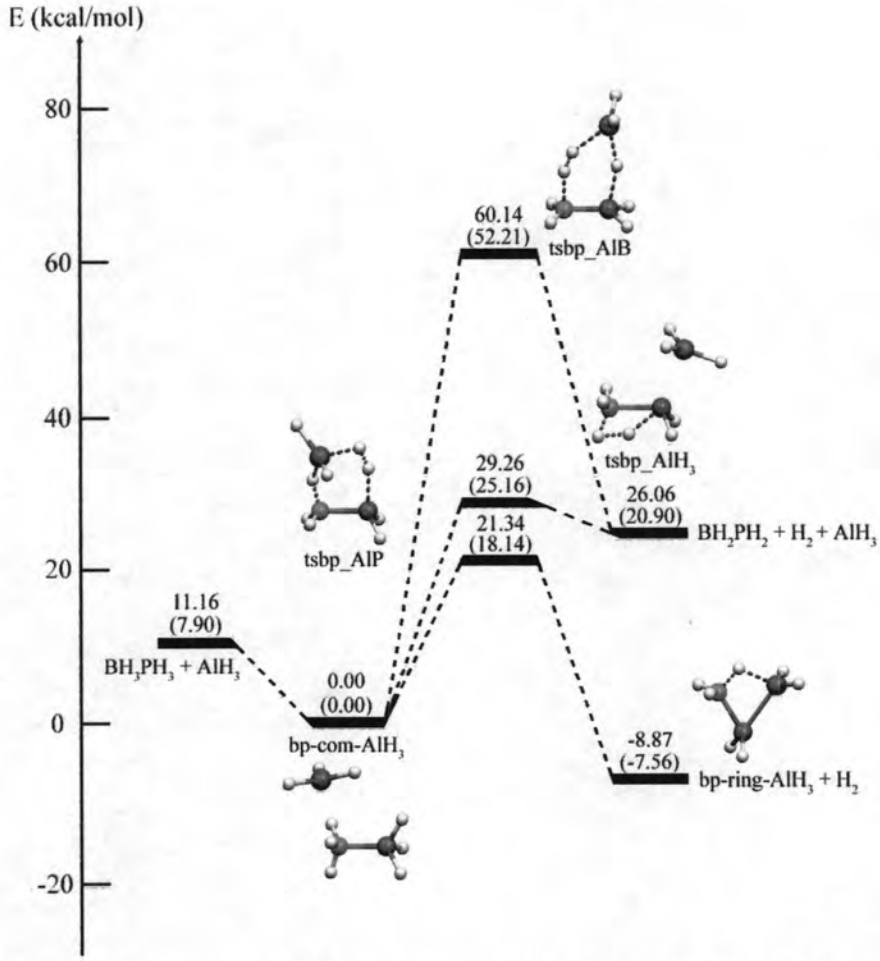

Figure 4.14 Reaction pathways for hydrogen release from BH_3PH_3 in the presence of AlH_3. Relative energies in kcal/mol computed at the MP2/6-311++G(d,p) and B3LYP/6-311++G(d,p) (in the parenthesis) levels of theory.

4.3.5 Reaction pathway for hydrogen release from BH_3PH_3 in the presence of PH_3

The energy profile for hydrogen release from BH_3PH_3 in the presence of PH_3 computed at the MP2/6-311++G(d,p) and B3LYP/6-311++G(d,p) (in the parenthesis) levels of theory are shown in Figure 4.15. Table 4.3 lists the relative energies, rate constants and thermodynamic properties of hydrogen release from BH_3PH_3 in the presence of PH_3. Figure 4.15 shows that the first step is the complexation of BH_3PH_3 and PH_3 resulting the **bp-com-PH_3**. The second step is composed of three reaction pathways via the transition states **tsbp_PB**, **tsbp_PH_3** and **tsbp_PP** as shown in Figure A-13. The activation energies of three pathways via **tsbp_PB**, **tsbp_PH_3** and **tsbp_PP** are 57.59, 52.45 and 66.61 kcal/mol, respectively. The most favorable

pathway is therefore the pathway via the transition state **tsbp_PH$_3$**. However the energy barrier via **tsbp_ PH$_3$** is higher than that found for **tsala** system, the PH_3 molecule cannot act as a catalyst for hydrogen release from borane phosphine with PH_3. Overall process gives the same separated products as BH_2PH_2, H_2 and PH_3. From all reaction energies via **tsbp_PB**, **tsbp_PH$_3$** and **tsbp_PP** are positive that indicate over all reaction become endothermic processes by 14.91 kcal/mol with respect the reactants.

Table 4.3 lists the calculated rate constants, including tunneling corrections, using TST for each process in this system from equations (3.43) and (3.44). The rate constants (k) via **tsbp_PB**, **tsbp_PH$_3$** and **tsbp_PP** are 1.71×10^{-31}, 2.82×10^{-26} and 8.32×10^{-39} s^{-1}, respectively. In addition, the tunneling factors (κ) and the equilibrium constants from equation (3.45) are listed in Tables B-3 and 4.3, respectively.

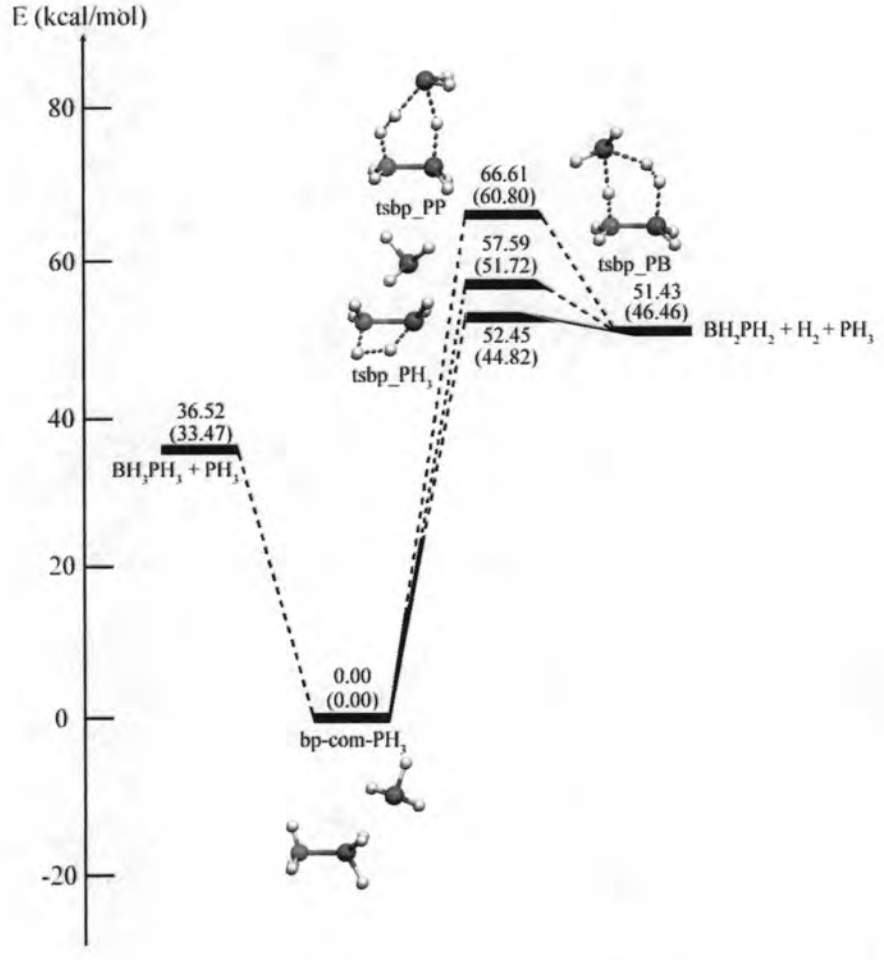

Figure 4.15 Reaction pathways for hydrogen release from BH_3PH_3 in the presence of PH_3. Relative energies in kcal/mol computed at the MP2/6-311++G(d,p) and B3LYP/6-311++G(d,p) (in the parenthesis) levels of theory.

The results show that the transition states **tsbp_NB** and **tsbp_AlP** are stabilized by the NH_3 and AlH_3, respectively and their structures are formed as the N···H···H···B, and Al···H···H···P configurations respectively. The reason is that the strong electrostatic attraction between the positively charged H_N (or H_P) atom and the negatively charged H_B (or H_{Al}) atom. The **tsbp_PH$_3$** is stabilized by the PH_3 as the most favorable transition state of which the structure of the four-membered framework is formed. This reason is that the PH_3 is the soft base of which the hydrogen atom is not released. As the hydrogen release reaction via the transition states, **tsbp_BH$_3$** and **tsbp_NB** afford the complex $PH_2BH_2BH_3$ and $PH_2BH_2NH_3$, respectively which the BH_3 and NH_3 cannot be released from its complex-state, therefore the BH_3 and NH_3 do not behave the catalyst for these reaction processes.

4.4 Molecular mechanism of hydrogen release from AlH_3PH_3 system

Table 4.4 lists the activation energies, rate constants and thermodynamic properties calculated at the MP2/6-311++G(d,p) and B3LYP/6-311++G(d,p) (in the parenthesis) levels of theory for hydrogen release from AlH_3PH_3 without and with the BH_3, NH_3, AlH_3 and PH_3. The reaction pathways for hydrogen release from AlH_3PH_3 system are presented in Figures 4.16-4.20.

4.4.1 Reaction pathway for synthesis of AlH_3PH_3 and hydrogen release from AlH_3PH_3

The schematic energy profile for hydrogen release from the alane phosphine is shown in Figure 4.16. The relative energies, rate constants and thermodynamic properties of hydrogen release from AlH_3PH_3 system computed at the MP2/6-311++G(d,p) and B3LYP/6-311++G(d,p) (in the parenthesis) levels of theory are listed in Table 4.4. The reaction pathway for hydrogen release from AlH_3PH_3 is composed of two reaction steps. The first step is the barrierless reaction and the spontaneous reaction. The second step is the rate-determining step. The transition state structure geometry, **tsalp** for loss of hydrogen from AlH_3PH_3 is similar to that for loss of hydrogen from BH_3NH_3, AlH_3NH_3 and BH_3PH_3. The shape and bond length for **tsalp** is shown in Figure A-1(d). The energy barrier of the transition-state

structure, **tsalp** was calculated to be 39.38 kcal/mol. For hydrogen release from AlH_3PH_3, the activation energy of hydrogen release reaction of AlH_3PH_3 higher than the reaction of AlH_3NH_3 by 9.85 kcal/mol. This reaction pathway is found to be an endothermic process.

We calculated the rate constants using the TST from equations (3.43) and (3.44). For hydrogen release from AlH_3PH_3, the rate constant is $k = 1.47\times10^{-15}$ s^{-1} which is lower than that calculated for AlH_3NH_3. In addition, the equilibrium constants that calculated from equation (3.45) are listed in Table 4.4 as $K = 3.32\times10^{1}$ and the tunneling factors (κ) are listed in Table B-4.

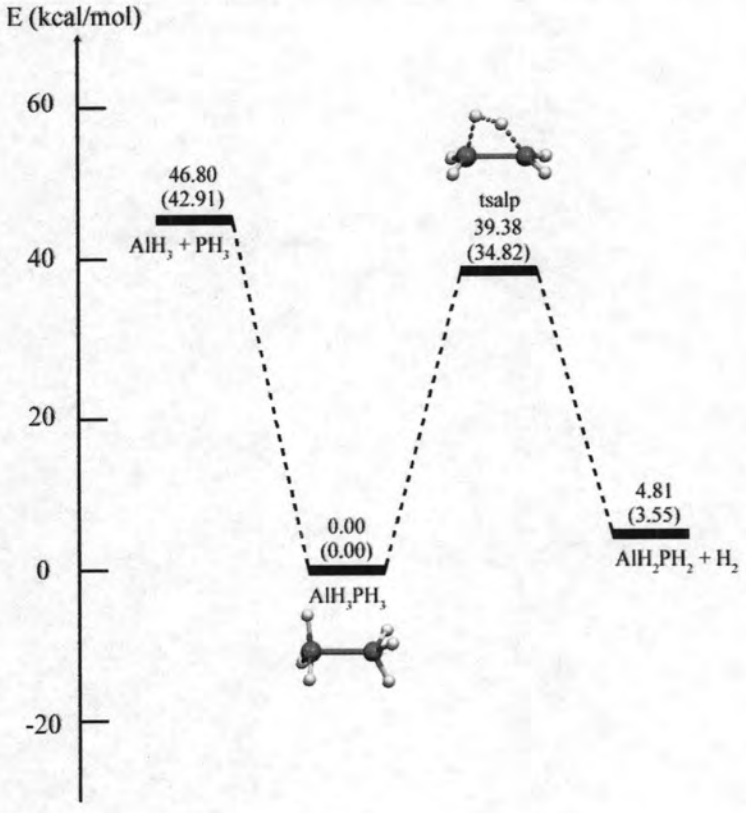

Figure 4.16 Reaction pathways for synthesis of AlH_3PH_3 and hydrogen release from AlH_3PH_3. Relative energies in kcal/mol computed at the MP2/6-311++G(d,p) and B3LYP/6-311++G(d,p) (in the parenthesis) levels of theory.

Table 4.4 Relative energies, rate constants and thermodynamic properties of hydrogen release from AlH_3PH_3 without and with BH_3, NH_3, AlH_3 or PH_3 catalyst, computed at the B3LYP/6-311++G(d,p) (in the parenthesis) and MP2/6-311++G(d,p) levels of theory

Reaction	$\Delta^{\ddagger}E^{a,b}$	$k_{298}{}^{c}$	ΔE^{a}	$\Delta H_{298}{}^{a}$	$\Delta G_{298}{}^{a}$	K_{298}
AlH_3PH_3 reactant:						
$AlH_3+PH_3 \rightarrow AlH_3PH_3$	-	-	-46.80	-47.56	-39.22	5.63×10^{28}
	-	-	(-42.91)	(-43.59)	(-35.39)	(8.82×10^{25})
$AlH_3PH_3 \rightarrow$ **tsalp** $\rightarrow AlH_2PH_2+H_2$	39.38	1.47×10^{-15}	4.81	6.22	-2.08	3.32×10^{1}
	(34.82)	(3.13×10^{-12})	(3.55)	(4.90)	(-3.29)	(2.59×10^{2})
AlH_3PH_3 and BH_3 reactants:						
$AlH_3PH_3+BH_3 \rightarrow AlH_3PH_3\cdots BH_3$	-	-	-31.49	-32.46	-23.60	1.99×10^{17}
	-	-	(-27.65)	(-28.61)	(-19.82)	(3.39×10^{14})
$AlH_3PH_3\cdots BH_3 \rightarrow$ **tsalp-BP** $\rightarrow PH_2AlH_2BH_3$(ring)$+H_2$	54.98	1.36×10^{-28}	-28.92	3.39	-2.64	8.58×10^{1}
	(51.66)	(1.03×10^{-25})	(-22.30)	(6.16)	(0.24)	(6.66×10^{-1})
$AlH_3PH_3\cdots BH_3 \rightarrow$ **tsalp-BH_3** $\rightarrow PH_2AlH_2BH_3$(ring)$+H_2$	46.89	6.73×10^{-22}	-28.92	3.39	-2.64	8.63×10^{1}
	(43.31)	(8.81×10^{-20})	(-22.30)	(6.16)	(0.24)	(6.66×10^{-1})
$AlH_3PH_3\cdots BH_3 \rightarrow$ **tsalp-BAl** $\rightarrow AlH_2PH_2+H_2+BH_3$	82.56	9.61×10^{-49}	4.81	38.68	21.52	1.67×10^{-16}
	(72.43)	(5.96×10^{-41})	(3.55)	(33.51)	(16.53)	(7.66×10^{-13})
AlH_3PH_3 and NH_3 reactants:						
$AlH_3PH_3+NH_3 \rightarrow AlH_3PH_3\cdots NH_3$	-	-	-4.90	-5.08	2.04	3.18×10^{-2}
	-	-	(-2.58)	(-2.98)	(3.94)	(1.30×10^{-3})
$AlH_3PH_3\cdots NH_3 \rightarrow$ **tsalp-NP** $\rightarrow AlH_2PH_2+H_2+NH_3$	95.38	2.34×10^{-58}	4.81	11.30	-4.12	1.04×10^{3}
	(85.34)	(1.31×10^{-51})	(3.55)	(7.88)	(-7.23)	(2.00×10^{5})
$AlH_3PH_3\cdots NH_3 \rightarrow$ **tsalp-NH_3** $\rightarrow AlH_2PH_2+H_2+NH_3$	28.26	1.14×10^{-9}	4.81	11.30	-4.12	1.04×10^{3}
	(24.70)	(3.08×10^{-7})	(3.55)	(7.88)	(-7.23)	(2.00×10^{5})
$AlH_3PH_3\cdots NH_3 \rightarrow$ **tsalp-NAl** $\rightarrow AlH_2PH_2+H_2+NH_3$	38.45	2.68×10^{-17}	4.81	11.30	-4.12	1.04×10^{3}
	(37.16)	(1.08×10^{-16})	(3.55)	(7.88)	(-7.23)	(2.00×10^{5})
AlH_3PH_3 and AlH_3 reactants:						
$AlH_3PH_3+AlH_3 \rightarrow AlH_3PH_3\cdots AlH_3$	-	-	-16.76	-17.50	-8.44	1.53×10^{6}
	-	-	(-13.54)	(-14.20)	(-5.42)	(9.48×10^{3})
$AlH_3PH_3\cdots AlH_3 \rightarrow$ **tsalp-AlP** $\rightarrow PH_2AlH_2AlH_3$(ring)$+H_2$	18.53	3.91×10^{-2}	-28.18	-10.39	-16.74	1.86×10^{12}
	(14.04)	(1.36×10^{2})	(-24.03)	(-9.51)	(-15.61)	(2.80×10^{11})
$AlH_3PH_3\cdots AlH_3 \rightarrow$ **tsalp-AlH_3** $\rightarrow PH_2AlH_2AlH_3+H_2$	35.10	5.83×10^{-14}	-26.19	-8.26	-15.48	2.24×10^{11}
	(30.52)	(8.34×10^{-11})	(-23.30)	(-8.73)	(-15.53)	(2.42×10^{11})
$AlH_3PH_3\cdots AlH_3 \rightarrow$ **tsalp-AlAl** $\rightarrow AlH_2PH_2+H_2+AlH_3$	65.08	1.29×10^{-35}	4.81	23.72	6.36	2.16×10^{-5}
	(55.09)	(1.97×10^{-28})	(3.55)	(19.10)	(2.13)	(2.73×10^{-2})
AlH_3PH_3 and PH_3 reactants:						
$AlH_3PH_3+PH_3 \rightarrow AlH_3PH_3\cdots PH_3$	-	-	-36.93	-36.59	-31.14	6.77×10^{22}
	-	-	(-33.57)	(-32.86)	(-30.04)	(1.05×10^{22})
$AlH_3PH_3\cdots PH_3 \rightarrow$ **tsalp-PP** $\rightarrow AlH_2PH_2+H_2+PH_3$	65.56	3.98×10^{-38}	4.81	42.81	29.07	4.91×10^{-22}
	(57.69)	(4.27×10^{-34})	(3.55)	(37.76)	(26.74)	(2.48×10^{-20})
$AlH_3PH_3\cdots PH_3 \rightarrow$ **tsalp-PH_3** $\rightarrow AlH_2PH_2+H_2+PH_3$	40.62	1.20×10^{-15}	4.81	42.81	29.07	4.91×10^{-22}
	(35.25)	(2.38×10^{-13})	(3.55)	(37.76)	(26.74)	(2.48×10^{-20})
$AlH_3PH_3\cdots PH_3 \rightarrow$ **tsalp-PAl** $\rightarrow AlH_2PH_2+H_2+PH_3$	51.42	1.13×10^{-26}	4.81	42.81	29.07	4.91×10^{-22}
	(38.71)	(1.14×10^{-19})	(3.55)	(37.76)	(26.74)	(2.48×10^{-20})

[a] In kcal/mol.
[b] Activation energy.
[c] In s^{-1}

4.4.2 Reaction pathway for hydrogen release from AlH_3PH_3 in the presence of BH_3

We have predicted the hydrogen release mechanism from alane phosphine involving an additional borane molecule. Table 4.4 lists the relative energies, rate constants and thermodynamic properties of hydrogen release from AlH_3PH_3 in the presence of BH_3 and the corresponding energy profile is illustrated in Figure 4.17. The reaction pathways for hydrogen release from AlH_3PH_3 are composed of two reaction steps. The first step is the complexation between AlH_3PH_3 and BH_3 resulting the **alp-com-BH_3**. The second step is composed of three transition-state structures via **tsalp_BP**, **tsalp_BH_3** and **tsalp_BAl** as shown in Figure A-14. The activation energies of three pathways via **tsalp_BP**, **tsalp_BH_3** and **tsalp_BAl** are 54.98, 46.98 and 82.56 kcal/mol, respectively. The process via **tsalp_BH_3** proceeds with the lowest energy. In the transition-state structures, **tsalp_BP** and **tsalp_BH_3** give the same separated products as the three-membered ring, **alp-ring-BH_3**. Even though the **tsalp_BH_3** is the lowest energy transition-state structure, the BH_3 molecule cannot play the role of a catalyst for hydrogen release from alane phosphine with BH_3. Because of the BH_3 molecule cannot be put back into the system.

We can apply the TST to predict the rate constant for hydrogen release of **alp-com-BH_3**, via **tsalp_BH_3**. By use of the equations (3.43) and (3.44), the TST rate constant of $k = 6.73\times10^{-22}$ s^{-1} is obtained. The tunneling factors (κ) and reaction constants of all hydrogen release compound systems are shown in Tables B-4 and 4.4, respectively. The equilibrium constants (K) calculated from equation (3.45) of the reaction via **tsalp_BH_3** and **tsalp_BAl** are 8.63×10^{1} and 1.67×10^{-16}, respectively which show that the product **alp-ring-BH_3** is more favorable product than the product AlH_2PH_2 because its structure is more stable than the product AlH_2PH_2.

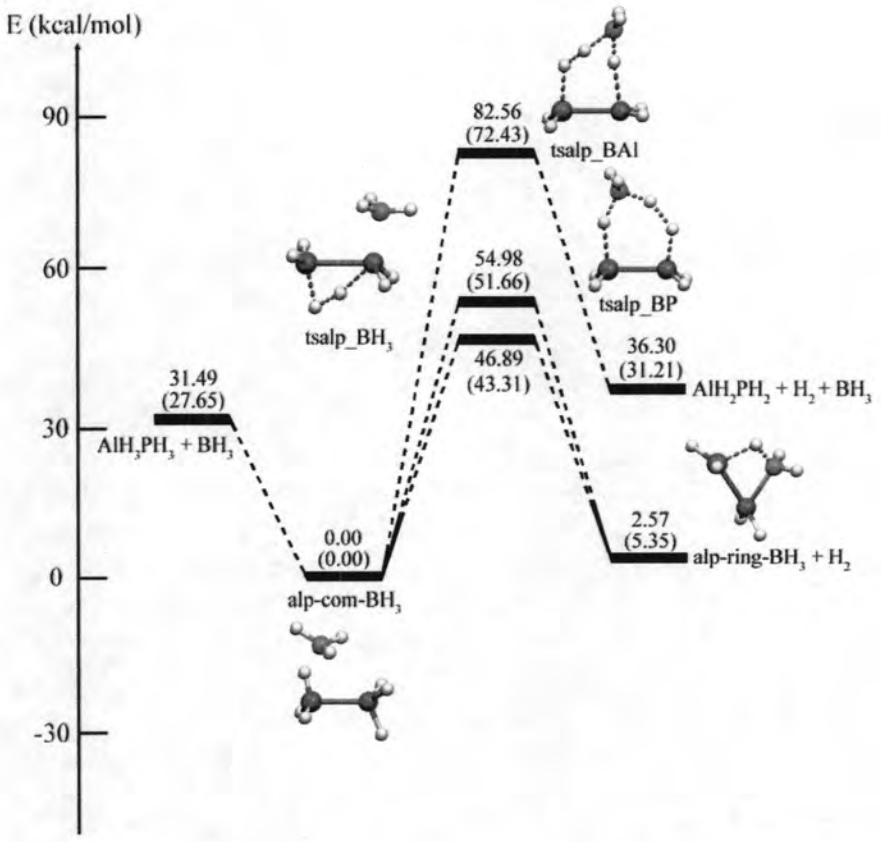

Figure 4.17 Reaction pathways for hydrogen release from AlH_3PH_3 in the presence of BH_3. Relative energies in kcal/mol computed at the MP2/6-311++G(d,p) and B3LYP/6-311++G(d,p) (in the parenthesis) levels of theory.

4.4.3 Reaction pathway for hydrogen release from AlH_3PH_3 in the presence of NH_3

For the AlH_3PH_3 + NH_3 reaction, the corresponding energy profile is illustrated in Figure 4.18 and Table 4.4 lists the relative energies, rate constants and thermodynamic properties of hydrogen release from AlH_3PH_3 in the presence of NH_3. The first step is the complexation of AlH_3PH_3 and PH_3 resulting the **alp-com-NH_3**. The second step is composed of three transition-state structures via **tsalp_NP**, **tsalp_NH_3** and **tsalp_NAl** as shown in Figure A-15. The activation energies of three pathways via **tsalp_NP**, **tsalp_NH_3** and **tsalp_NAl** are 95.38, 38.45 and 28.26 kcal/mol, respectively. The **tsalp_NH_3** is the lowest energy transition structure which represents a reduction of 11.12 kcal/mol with respect to the energy barrier of 39.38 kcal/mol in the AlH_3PH_3 monomer via **tsalp**, see Figure A-1(d). All processes via three transition state structures give the same separated products as AlH_2PH_2, H_2 and

NH_3. From all reaction energies via **tsalp_NP**, **tsalp_NH$_3$** and **tsalp_NAl** are positive that indicate over all reaction become endothermic processes by 4.81kcal/mol with respect the reactants.

The rate constants of these processes, we can evaluate by equations (3.43) and (3.44). The rate constants (k) via **tsalp_NP**, **tsalp_NH$_3$** and **tsalp_NAl** are 2.34×10^{-58}, 1.14×10^{-9} and 2.68×10^{-17} s^{-1}, respectively. In addition, the tunneling factors (κ) and reaction constants of all hydrogen storage compound systems are shown in Tables B-4 and 4.4, respectively.

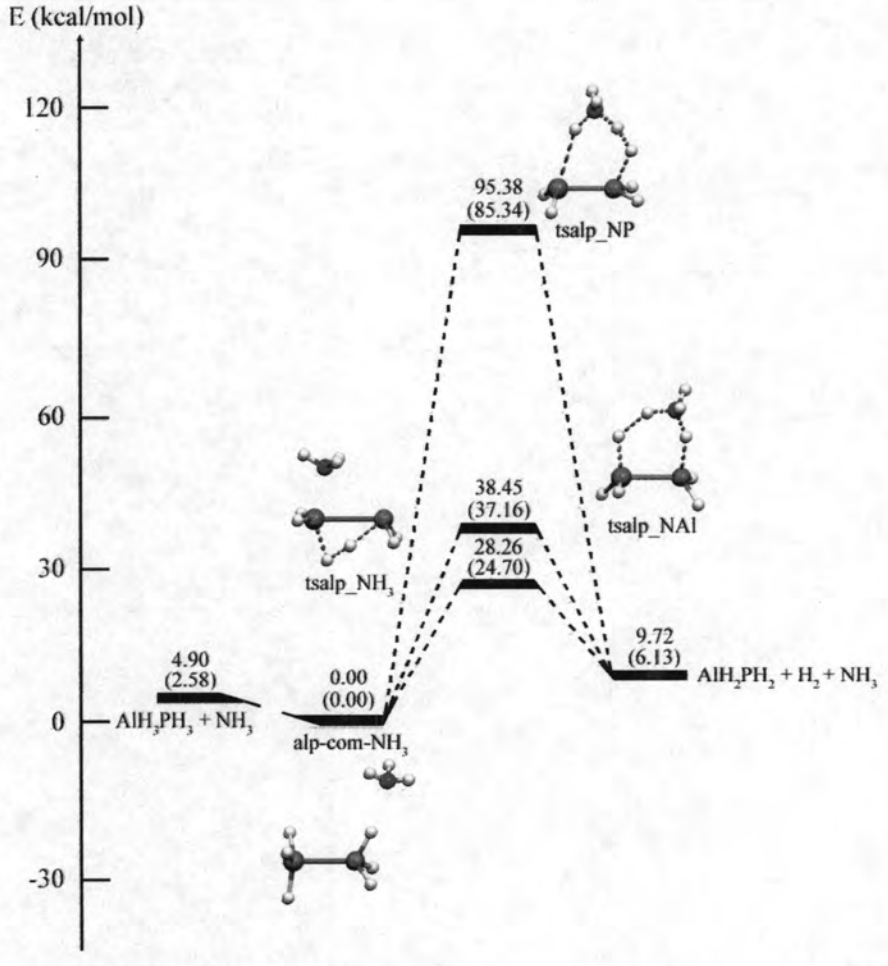

Figure 4.18 Reaction pathways for hydrogen release from AlH_3PH_3 in the presence of NH_3. Relative energies in kcal/mol computed at the MP2/6-311++G(d,p) and B3LYP/6-311++G(d,p) (in the parenthesis) levels of theory.

4.4.4 Reaction pathway for hydrogen release from AlH_3PH_3 in the presence of AlH_3

The corresponding energy profile is illustrated in Figure 4.19 and Table 4.4 lists the relative energies, rate constants and thermodynamic properties of hydrogen release from AlH_3PH_3 in the presence of AlH_3. For the AlH_3PH_3 + AlH_3 reaction, we located three different transition structures such as the AlH_3PH_3 +BH_3 reaction. The shape and characteristics of the stationary points involving AlH_3 are similar in many respects to those involving BH_3 discussed above. The first step, the complex **alp-com-AlH_3** between AlH_3PH_3 and AlH_3 is formed. The second step is composed of three transition-state structures via **tsalp_AlP**, **tsalp_AlH_3** and **tsalp_AlAl** as shown in Figure A-16. The activation energies of three pathways via **tsalp_AlP**, **tsalp_AlH_3** and **tsalp_AlAl** are 18.53, 35.10 and 65.08 kcal/mol, respectively. In transition-state structure, **tsalp_AlH_3** has the separated products as $PH_2AlH_2AlH_3$ and H_2. The most favorable pathway is therefore the pathway via the transition state **tsalp_AlP**. The product from this process is **alp-ring-AlH_3** and H_2. Although the hydrogen release from AlH_3PH_3 with the AlH_3 via **tsalp_AlP** is lowest energy, the AlH_3 molecule cannot serve as a catalyst for hydrogen release from alane phosphine with AlH_3. Due to the AlH_3 molecule cannot be put back into the system.

The rate constants of these processes, we can evaluate by equations (3.43) and (3.44). The rate constants (k) via **tsalp_AlP**, **tsalp_AlH_3** and **tsalp_AlAl** are 3.91×10^{-2}, 5.83×10^{-14} and 1.29×10^{-35} s^{-1}, respectively. In addition, the tunneling factors (κ) are listed in Table B-4 and the equilibrium constants can be calculated by equation (3.45) as shown in Table 4.4. For the hydrogen release reaction via **tsalp_AlP** and **tsalp_AlAl**, the equilibrium constants (K) are 1.86×10^{12} and 2.16×10^{-5}, respectively. It is found that the product **alp-ring-AlH_3** is more favorable product than the product AlH_2PH_2 because its structure is more stable than the product AlH_2PH_2.

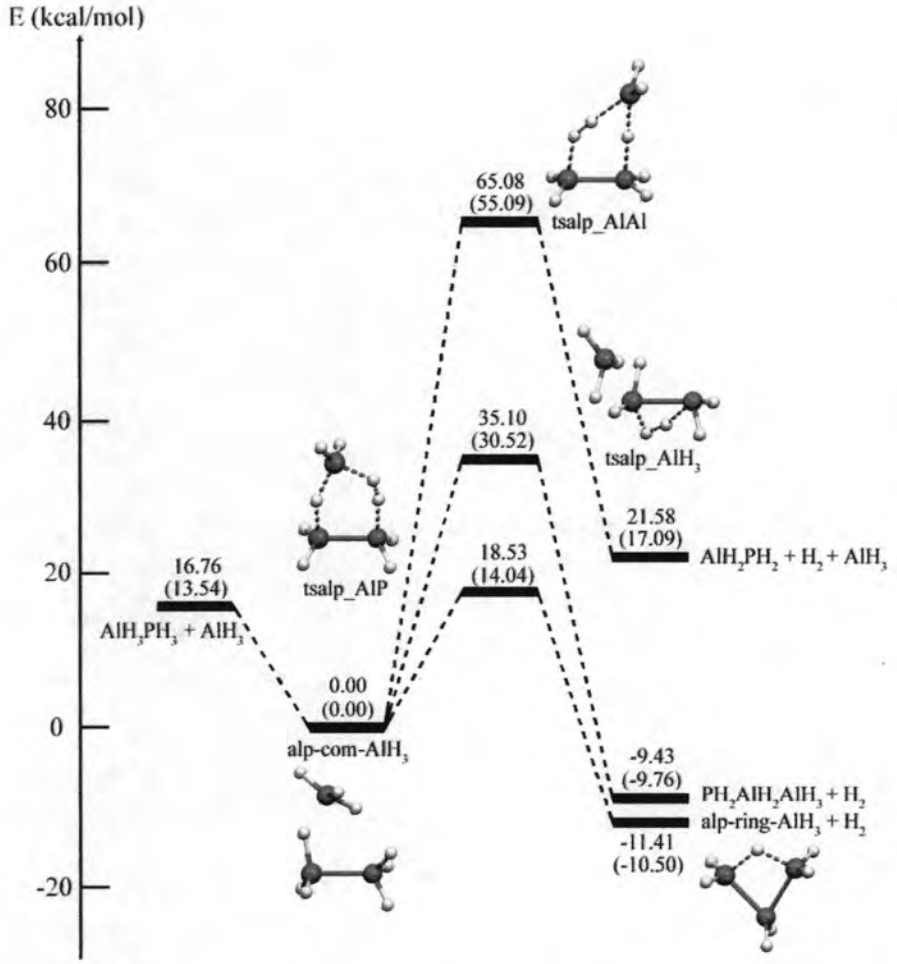

Figure 4.19 Reaction pathways for hydrogen release from AlH_3PH_3 in the presence of AlH_3. Relative energies in kcal/mol computed at the MP2/6-311++G(d,p) and B3LYP/6-311++G(d,p) (in the parenthesis) levels of theory.

4.4.5 Reaction pathway for hydrogen release from AlH_3PH_3 in the presence of PH_3

Table 4.4 lists the relative energies, rate constants and thermodynamic properties of hydrogen release from AlH_3PH_3 with the presence of PH_3 computed at the MP2/6-311++G(d,p) and B3LYP/6-311++G(d,p) (in the parenthesis) levels of theory. The schematic energy profile for hydrogen release from the alane phosphine with PH_3 is shown in Figure 4.20. The reaction pathways for hydrogen release from AlH_3PH_3 with PH_3 are composed of two reaction steps. The complex **alp-com-PH_3** between AlH_3PH_3 and PH_3 is initially formed and is -36.93 kcal/mol more stable than the AlH_3PH_3 + PH_3. Starting from **alp-com-PH_3**, three transition-state structures have

been located, each representing a different type of hydrogen elimination are also shown in Figure A-17. Normal modes for the imaginary frequencies of three transition states are listed in Table B-4. The activation energies of three pathways in the second step via **tsalp_PP**, **tsalp_PH$_3$** and **tsalp_PAl** are 65.56, 40.62 and 51.42 kcal/mol, respectively. The most favorable pathway is therefore the pathway via the transition state **tsalp_ PH$_3$**. Although the **tsalp_PH$_3$** is the lowest energy transition structure, the energy barrier via **tsalp_ PH$_3$** is higher than that found for **tsalp** system without catalyst. As a result, the PH_3 molecule cannot play the role of a catalyst for hydrogen release from alane phosphine with phosphine. Overall process gives the same separated products as AlH_2PH_2, H_2 and PH_3. From all reaction energies via **tsalp_PP**, **tsalp_PH$_3$** and **tsalp_PAl** are positive which indicate that the overall reaction become endothermic processes by 4.81 kcal/mol with respect the reactants.

The rate constants of these processes can be calculated by equations (3.43) and (3.44). The rate constants (k) via **tsalp_PP**, **tsalp_PH$_3$** and **tsalp_PAl** are 3.98×10^{-38}, 1.20×10^{-15} and 1.13×10^{-26} s^{-1}, respectively. Furthermore, the tunneling factors (κ) are listed in Table B-4, and equilibrium constants are shown in Table 4.4.

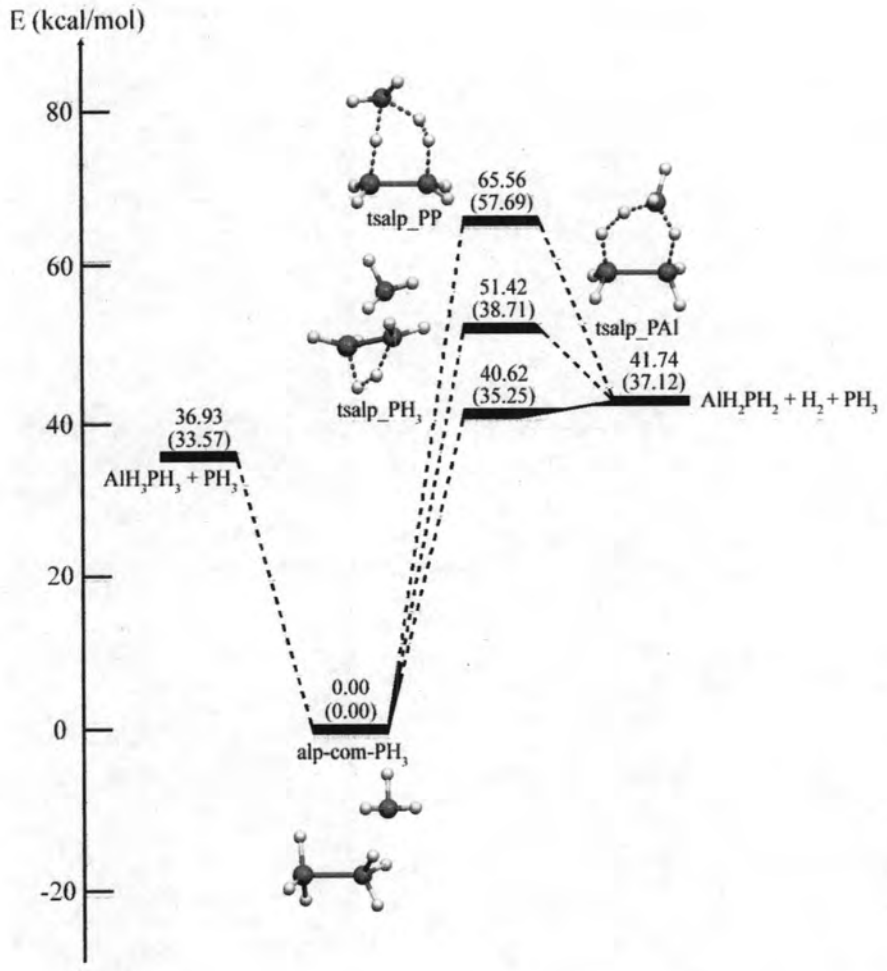

Figure 4.20 Reaction pathways for hydrogen release from AlH_3PH_3 in the presence of PH_3. Relative energies in kcal/mol computed at the MP2/6-311++G(d,p) and B3LYP/6-311++G(d,p) (in the parenthesis) levels of theory.

The results show that the transition state **tsalp_AlP** is stabilized by the AlH_3 and its structure is formed as the Al···H···H···P configuration. The reason is that the strong electrostatic attraction between the positively charged H_P atom and the negatively charged or H_{Al} atom. As the hydrogen release reaction via the transition states, **tsalp_BH3** and **tsalp_AlP** afford the **alp-ring-BH3** and **alp-ring-AlH3**, respectively which the BH_3 and AlH_3 are never released from its complex-state, therefore these reaction pathways is not considered as the hydrogen energy source.

4.5 The catalytic ability of BH_3, NH_3, AlH_3 and PH_3 in the reaction of hydrogen storage compounds

The collection rate constants for hydrogen release reactions of BH_3NH_3, AlH_3NH_3, BH_3PH_3 and AlH_3PH_3 using the BH_3, NH_3, AlH_3 or PH_3 catalysts is tabulated in Table 4.5.

Based on the catalytic reactions of hydrogen release from the hydrogen storage compounds, the relation between their rate constants and their corresponding catalysts is plotted as shown in Figure 4.21.

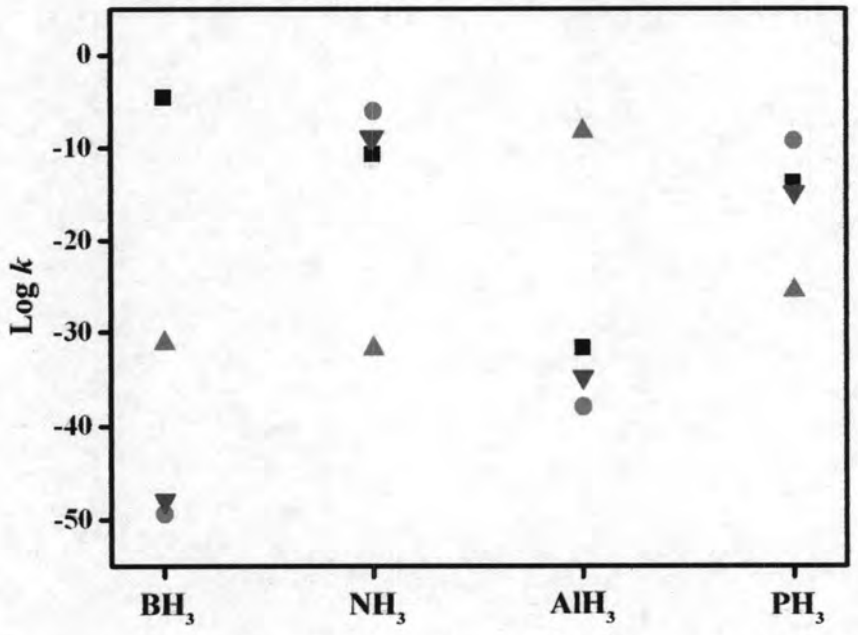

Figure 4.21 Relation between log k of hydrogen release reactions of BH_3NH_3 (■), AlH_3NH_3 (●), BH_3PH_3 (▲) and AlH_3PH_3 (▼) and various BH_3, NH_3, AlH_3 and PH_3 catalyst.

Figure 4.21 shows that the BH_3, NH_3 and AlH_3 compounds are the best catalysts in the hydrogen release reactions of BH_3NH_3, AlH_3NH_3 and BH_3PH_3, respectively. For the hydrogen release reaction of AlH_3PH_3, the NH_3 compound is found to be the best catalyst. The PH_3 does not behave as a catalyst in any studied reaction. As the PH_3 is the soft base, its hydrogen atoms dislike to be abstracted. Due to the large size of the PH_3, its molecular structure may destabilize the transition state of their hydrogen release reactions.

Table 4.5 Rate constants (k) of the hydrogen release reactions of hydrogen storage compounds in the presence of the BH_3, NH_3, AlH_3 or PH_3, computed at the B3LYP/6-311++G(d,p) (in the parenthesis) and MP2/6-311++G(d,p) levels of theory

Catalyst	Rate constant, s^{-1}											
	BH_3NH_3			AlH_3NH_3			BH_3PH_3			AlH_3PH_3		
BH_3	**tsba_BN** [a,b]	**tsba_BH_3**	**tsba_BN**	**tsala_BH_3** [a]	**tsala_BN**	**tsala_BAl** [b]	**tsbp_BH_3** [a]	**tsbp_BP**	**tsbp_BB** [b]	**tsalp_BH_3** [a]	**tsalp_BP**	**tsalp_BAl** [b]
	2.37×10^{-5}	2.25×10^{-20}	3.36×10^{-35}	7.32×10^{-10}	1.92×10^{-21}	3.23×10^{-50}	2.29×10^{-3}	1.08×10^{-10}	6.01×10^{-32}	6.73×10^{-22}	1.36×10^{-28}	9.61×10^{-49}
	(1.95×10^{-3})	(8.11×10^{-21})	(2.55×10^{-30})	(3.58×10^{-8})	(3.40×10^{-17})	(3.45×10^{-43})	(9.89×10^{-2})	(3.99×10^{-8})	(2.24×10^{-28})	(8.81×10^{-20})	(1.03×10^{-25})	(5.96×10^{-41})
NH_3	**tsba_NB** [a,b]	**tsba_NH_3**	**tsba_NN**	**tsala_NAl** [a,b]	**tsba_NH_3**	**tsala_NN**	**tsbp_NB** [a]	**tsbp_NH_3** [b]	**tsbp_NP**	**tsalp_NH_3** [a,b]	**tsalp_NAl**	**tsalp_NP**
	1.81×10^{-11}	1.53×10^{-16}	5.34×10^{-67}	6.87×10^{-7}	1.10×10^{-11}	6.00×10^{-85}	1.16×10^{-19}	1.35×10^{-32}	1.79×10^{-50}	1.14×10^{-9}	2.68×10^{-17}	2.34×10^{-58}
	(4.05×10^{-10})	(7.75×10^{-15})	(1.66×10^{-61})	(1.21×10^{-6})	(8.85×10^{-10})	(1.81×10^{-76})	(1.26×10^{-24})	(1.12×10^{-30})	(9.82×10^{-48})	(3.08×10^{-7})	(1.08×10^{-16})	(1.31×10^{-51})
AlH_3	**tsba_AlN** [a]	**tsba_AlH_3**	**tsba_AlB** [b]	**tsala_AlN** [a]	**tsba_AlH_3**	**tsala_AlAl** [b]	**tsbp_AlP** [a]	**tsbp_AlH_3** [b]	**tsbp_AlB**	**tsalp_AlP** [a]	**tsalp_AlH_3**	**tsalp_AlAl** [b]
	1.30×10^{-1}	6.66×10^{-19}	2.00×10^{-32}	5.64	8.61×10^{-10}	8.91×10^{-39}	4.39×10^{-4}	4.17×10^{-9}	3.29×10^{-32}	3.91×10^{-2}	5.83×10^{-14}	1.29×10^{-35}
	(9.27×10^{-1})	(2.50×10^{-18})	(1.28×10^{-27})	(6.18×10^{4})	(5.39×10^{-9})	(1.09×10^{-32})	(1.04×10^{-1})	(2.83×10^{-6})	(2.52×10^{-26})	(1.36×10^{2})	(8.34×10^{-11})	(1.97×10^{-28})
PH_3	**tsba_PH_3** [a,b]	**tsba_PB**	**tsba_PN**	**tsala_PH_3** [a,b]	**tsala_PAl**	**tsala_PN**	**tsbp_PH_3** [a,b]	**tsbp_PB**	**tsbp_PP**	**tsalp_PH_3** [a,b]	**tsalp_PAl**	**tsalp_PP**
	1.36×10^{-14}	2.07×10^{-22}	3.37×10^{-34}	4.71×10^{-10}	4.61×10^{-23}	4.01×10^{-35}	2.82×10^{-26}	1.71×10^{-31}	8.32×10^{-39}	1.20×10^{-15}	1.13×10^{-26}	3.98×10^{-38}
	(5.23×10^{-12})	(1.64×10^{-24})	(1.03×10^{-29})	(1.36×10^{-8})	(9.50×10^{-16})	(4.17×10^{-32})	(6.87×10^{-21})	(3.56×10^{-29})	(2.78×10^{-36})	(2.38×10^{-13})	(1.14×10^{-19})	(4.27×10^{-34})

[a] The highest rate constants for each system of hydrogen storage compounds.

[b] The highest rate constants for each system of hydrogen storage compounds based on the BH_3, NH_3, AlH_3 and PH_3 as catalyst.